U.S. DEPARTMENT OF COMMERCE
National Technical Information Service
PB-297 393

Effect of Diethylhydroxylamine on Smog Chamber Irradiations

Northrop Services, Inc, Research Triangle Park, NC

Prepared for

Environmental Sciences Research Lab, Research Triangle Park, NC

Apr 79

United States
Environmental Protection
Agency

Environmental Sciences Research
Laboratory
Research Triangle Park NC 27711

EPA-600/3-79-040
April 1979

Research and Development

EPA

Effect of Diethylhydroxylamine on Smog Chamber Irradiations

PB 297393

REPRODUCED BY
NATIONAL TECHNICAL
INFORMATION SERVICE
U. S. DEPARTMENT OF COMMERCE
SPRINGFIELD, VA. 22161

RESEARCH REPORTING SERIES

Research reports of the Office of Research and Development, U.S. Environmental Protection Agency, have been grouped into nine series. These nine broad categories were established to facilitate further development and application of environmental technology. Elimination of traditional grouping was consciously planned to foster technology transfer and a maximum interface in related fields. The nine series are:

1. Environmental Health Effects Research
2. Environmental Protection Technology
3. Ecological Research
4. Environmental Monitoring
5. Socioeconomic Environmental Studies
6. Scientific and Technical Assessment Reports (STAR)
7. Interagency Energy-Environment Research and Development
8. "Special" Reports
9. Miscellaneous Reports

This report has been assigned to the ECOLOGICAL RESEARCH series. This series describes research on the effects of pollution on humans, plant and animal species, and materials. Problems are assessed for their long- and short-term influences. Investigations include formation, transport, and pathway studies to determine the fate of pollutants and their effects. This work provides the technical basis for setting standards to minimize undesirable changes in living organisms in the aquatic, terrestrial, and atmospheric environments.

This document is available to the public through the National Technical Information Service, Springfield, Virginia 22161.

TECHNICAL REPORT DATA
(Please read Instructions on the reverse before completing)

1. REPORT NO. EPA-600/3-79-040	2.
3. RECIPIENT'S ACCESSION NO. PB297393	
4. TITLE AND SUBTITLE: EFFECT OF DIETHYLHYDROXYLAMINE ON SMOG CHAMBER IRRADIATIONS	5. REPORT DATE: April 1979
	6. PERFORMING ORGANIZATION CODE
7. AUTHOR(S): L. T. Cupitt, E. W. Corse	8. PERFORMING ORGANIZATION REPORT NO.
9. PERFORMING ORGANIZATION NAME AND ADDRESS: Northrop Services Inc., Environmental Sciences Center, Research Triangle Park, North Carolina 27709	10. PROGRAM ELEMENT NO. 1AA603 AC-02 (FY-78)
	11. CONTRACT/GRANT NO. Contract no. 68-02-2566
12. SPONSORING AGENCY NAME AND ADDRESS: Environmental Sciences Research Laboratory-RTP, NC, Office of Research and Development, U.S. Environmental Protection Agency, Research Triangle Park, North Carolina 27711	13. TYPE OF REPORT AND PERIOD COVERED: Final
	14. SPONSORING AGENCY CODE: EPA/600/09
15. SUPPLEMENTARY NOTES	

16. ABSTRACT

The addition of diethylhydroxylamine (DEHA) to the urban atmosphere had been suggested as a means of preventing photochemical smog. Smog chamber studies were carried out to investigate the photochemical smog formation characteristics of irradiated hydrocarbon-nitrogen oxides - DEHA mixtures. Propylene and n-butane were the hydrocarbons used. The effects of DEHA upon ozone formation, aerosol formation, peroxyacetyl nitrate formation, nitric oxide-to-NO_x conversion, and hydrocarbon consumed are described. The rate constant for the reaction

$$DEHA + OH \rightarrow \text{products}$$

was estimated as $4.1 \pm 3.4 \times 10^5$ $ppm^{-1}min^{-1}$. Possible reaction schemes for DEHA in the photochemical smog mechanism are discussed.

The addition of DEHA to a HC/NO_x system inhibits the conversion of NO to NO_2 during the initial minutes of irradiation, but after continued irradiation accelerates this conversion.

17. KEY WORDS AND DOCUMENT ANALYSIS

a. DESCRIPTORS	b. IDENTIFIERS/OPEN ENDED TERMS	c. COSATI Field/Group
* Air pollution		13B
* Hydroxyamine		07B
Nitrogen oxides		07C
Propylene		07E
Butanes		14B
* Photochemical reactions		
Test chambers		

18. DISTRIBUTION STATEMENT: RELEASE TO PUBLIC	19. SECURITY CLASS *(This Report)*: UNCLASSIFIED	21. NO. OF PAGES
	20. SECURITY CLASS *(This page)*: UNCLASSIFIED	22. PRICE

EPA Form 2220-1 (9-73)

EPA-600/3-79-040
April 1979

EFFECT OF DIETHYLHYDROXYLAMINE ON SMOG CHAMBER IRRADIATIONS

by

Larry T. Cupitt
Eric W. Corse

Environmental Science and Emissions Research
Northrop Services, Inc.
Environmental Sciences Center
Post Office Box 12313
Research Triangle Park, North Carolina 27709

Contract No. 68-02-2566

Project Officer

ph J. Bufalini

Atmospheric Chemistry and Physics Division
Environmental Sciences Research Laboratory
U.S. Environmental Protection Agency
Research Triangle Park, North Carolina 27711

ENVIRONMENTAL SCIENCES RESEARCH LABORATORY
OFFICE OF RESEARCH AND DEVELOPMENT
U.S. ENVIRONMENTAL PROTECTION AGENCY
RESEARCH TRIANGLE PARK, NORTH CAROLINA 27711

DISCLAIMER

This report has been reviewed by the Environmental Sciences Research Laboratory, U.S. Environmental Protection Agency, and approved for publication. Approval does not signify that the contents necessarily reflect the views and policies of the U.S. Environmental Protection Agency, nor does mention of trade names or commercial products constitute endorsement or recommendation for use.

ABSTRACT

The addition of diethylhydroxylamine (DEHA) to the urban atmosphere had been suggested as a means of preventing photochemical smog. Smog chamber studies were carried out to investigate the photochemical smog formation characteristics of irradiated hydrocarbon-nitrogen oxides - DEHA mixtures. Propylene and n-butane were the hydrocarbons used. The effects of DEHA upon ozone formation, aerosol formation, peroxyacetyl nitrate formation, nitric oxide-to-NO_x conversion, and hydrocarbon consumed are described. The rate constant for the reaction

$$\text{DEHA} + \text{OH} \longrightarrow \text{products}$$

was estimated as $4.1 \pm 3.4 \times 10^5$ $ppm^{-1}min^{-1}$. Possible reaction schemes for DEHA in the photochemical smog mechanism are discussed.

The addition of DEHA to a HC/NO_x system inhibits the conversion of NO to NO_2 during the initial minutes of irradiation, but after continued irradiation accelerates this conversion.

This report is submitted in fulfillment of Contract No. 68-02-2566 by Northrop Services, Inc., under the sponsorship of the U.S. Environmental Protection Agency. This work covers a period from November, 1976 to December, 1977, and work was completed as of May 1978.

CONTENTS

Abstract iii
Figures. vi
Tables ix
Abbreviations and Symbols. x
Acknowledgments. xii

1. Introduction. 1
2. Experimental. 2
3. Results 5
4. Discussion. 26
   DEHA Effects on Aspects of Smog Formation 26
   Potential Mechanisms to Explain DEHA Effects on Smog Formation 31
5. Conclusions 36

References 38
Appendix 40

Preceding page blank

FIGURES

Number		Page
1	Schematic diagram of chamber and support equipment	3
2	Reaction profiles of DEHA-NO_x system	8
3	Reaction profiles of 0.25 ppm propylene-NO_x system	9
4	Reaction profiles of ~0.25 ppm propylene-NO_x-DEHA system	10
5	Reaction profiles of 0.5 ppm propylene-NO_x system.	11
6	Reaction profiles of ~0.5 ppm propylene-NO_x-DEHA system	12
7	Reaction profiles of 5.0 ppm propylene-NO_x system	13
8	Reaction profiles of ~5 ppm propylene-NO_x-DEHA system.	14
9	Reaction profiles of ~0.5 ppm n-butane-NO_x system	15
10	Reaction profiles of ≈0.5 ppm n-butane-NO_x-DEHA system	16
11	Reaction profiles of 5.0 ppm n-butane-NO_x system	17
12	Reaction profiles of ~5 ppm n-butane-NO_x-DEHA system	18
13	Reaction profiles of ~15 ppm n-butane-NO_x system	19
14	Reaction profiles of 15.0 ppm n-butane-NO_x-DEHA system	20
15	Effect of changes of $[DEHA]_o/[HC]_o$ on manifestations of "smog" for an initial HC concentration of ~0.25 ppm propylene	22
16	"Smog" manifestations for an initial HC concentration of ~0.5 ppm propylene	23
17	Effect of $[DEHA]_o/[HC]_o$ on "smog" manifestations for an initial HC concentration of ~5 ppm propylene	24
18	Aerosol formation data versus time for runs with and without DEHA	25

Number		Page
19	Possible reaction mechanism for DEHA	32
20	Simulation profiles for HC, NO, NO_2, O_3, and DEHA predicted by kinetic model	34
A-1	Reaction profiles of DEHA-NO_x system	41
A-2	Reaction profiles of 0.25 ppm propylene-NO_x system	42
A-3	Reaction profiles of 0.25 ppm propylene-NO_x system	43
A-4	Reaction profiles of 0.24 ppm propylene-NO_x-DEHA system.	44
A-5	Reaction profiles of 0.26 ppm propylene-NO_x-DEHA system.	45
A-6	Reaction profiles of 0.30 ppm propylene-NO_x-DEHA system.	46
A-7	Reaction profiles of 0.30 ppm propylene-NO_x-DEHA system.	47
A-8	Reaction profiles of 0.49 ppm propylene-NO_x system	48
A-9	Reaction profiles of 0.48 ppm propylene-NO_x system	49
A-10	Reaction profiles of 0.50 ppm propylene-NO_x system	50
A-11	Reaction profiles of 0.60 ppm propylene-NO_x-DEHA system	51
A-12	Reaction profiles of 0.50 ppm propylene-NO_x-DEHA system	52
A-13	Reaction profiles of 0.54 ppm propylene-NO_x system	53
A-14	Reaction profiles of 0.47 ppm propylene-NO_x system	54
A-15	Reaction profiles of 0.50 ppm propylene-NO_x-DEHA system.	55
A-16	Reaction profiles of 0.54 ppm propylene-NO_x system	56
A-17	Reaction profiles of 0.55 ppm propylene-NO_x system	57
A-18	Reaction profiles of 0.54 ppm propylene-NO_x-DEHA system.	58
A-19	Reaction profiles of 0.47 ppm propylene-NO_x system	59
A-20	Reaction profiles of 0.52 ppm propylene-NO_x system	60
A-21	Reaction profiles of 0.52 ppm propylene-NO_x system	61
A-22	Reaction profiles of 0.50 ppm propylene-NO_x system	62
A-23	Reaction profiles of 0.55 ppm propylene-NO_x-DEHA system.	63

Number		Page
A-24	Reaction profiles of 5.0 ppm propylene-NO_x system	64
A-25	Reaction profiles of 5.2 ppm propylene-NO_x system	65
A-26	Reaction profiles of 5.1 ppm propylene-NO_x system	66
A-27	Reaction profiles of 5.3 ppm propylene-NO_x-DEHA system . . .	67
A-28	Reaction profiles of 4.7 ppm propylene-NO_x-DEHA system . . .	68
A-29	Reaction profiles of 4.9 ppm propylene-NO_x-DEHA system . . .	69
A-30	Reaction profiles of 5.0 ppm propylene-NO_x-DEHA system . . .	70
A-31	Reaction profiles of 4.7 ppm propylene-NO_x-DEHA system . . .	71
A-32	Reaction profiles of 0.49 ppm n-butane-NO_x system	72
A-33	Reaction profiles of 0.59 ppm n-butane-NO_x system	73
A-34	Reaction profiles of 0.48 ppm n-butane-NO_x system.	74
A-35	Reaction profiles of 0.46 ppm n-butane-NO_x-DEHA system . . .	75
A-36	Reaction profiles of 0.55 ppm n-butane-NO_x-DEHA system . . .	76
A-37	Reaction profiles of 0.59 ppm n-butane-NO_x-DEHA system . . .	77
A-38	Reaction profiles of 4.9 ppm n-butane-NO_x system	78
A-39	Reaction profiles of 4.9 ppm n-butane-NO_x system	79
A-40	Reaction profiles of 4.3 ppm n-butane-NO_x-DEHA system . . .	80
A-41	Reaction profiles of 4.7 ppm n-butane-NO_x-DEHA system . . .	81
A-42	Reaction profiles of 4.8 ppm n-butane-NO_x-DEHA system. . . .	82
A-43	Reaction profiles of 14.0 ppm n-butane-NO_x system	83
A-44	Reaction profiles of 14.3 ppm n-butane-NO_x system	84
A-45	Reaction profiles of 13.6 ppm n-butane-NO_x-DEHA system . . .	85
A-46	Reaction profiles of 13.5 ppm n-butane-NO_x-DEHA system . . .	86
A-47	Reaction profiles of NO_x system	87

TABLES

Number		Page
1	Results of Irradiation of HC/NO_x/DEHA Mixture Using Propylene.	21

ABBREVIATIONS AND SYMBOLS

ABBREVIATIONS

approx.	— approximately
ARB	— Aerosol Research Branch
°C	— degree Celsius
cm	— centimeter
DVM	— digital voltmeter
EAA	— electrical aerosol analyzer
EPA	— U.S. Environmental Protection Agency
ERC	— Environmental Research Center
°F	— degree Fahrenheit
FID	— flame ionization detection
ft	— foot
FTIR	— Fourier transform infrared spectroscopy
GC	— gas chromatograph
hr	— hour
in	— inch
IR	— infrared
l	— liter
MCA	— multichannel analyzer
µm	— micrometer
min	— minute
MS	— mass spectrometer
NBS	— National Bureau of Standards
NSI	— Northrop Services, Inc.
OPC	— optical particle counter
ppb	— part per billion
ppm	— part per million

RTP	— Research Triangle Park, North Carolina
sec	— second

SYMBOLS

CH_3CHO	— acetaldehyde (ALD2) (C_2H_4O)
$CH_3CH_2NO_2$	— nitroethane ($EtNO_2$)
C_2H_4	— ethylene
$C_2H_5NO_2$	— ethyl nitrite (NET) (nitroethane)
C_2H_5OH	— ethanol
$C_2H_5ONO_2$	— ethyl nitrate (NIT)
C_3H_6	— propylene
C_4H_{10}	— n-butane
DEHA	— diethylhydroxylamine
DENO	— $(C_2H_5)_2$-N-O·
HC	— hydrocarbon
HNO_3	— nitric acid
HONO	— nitrous acid
HO_2	— hydroperoxide
H_2	— hydrogen
H_2O	— water
NO	— nitric oxide
NO_2	— nitrogen dioxide
NO_x	— nitrogen oxides
N_2	— nitrogen
N_2O	— nitrous oxide (N2O)
O	— atomic oxygen
OH	— hydroxyl radical
O_2	— oxygen
O_3	— ozone
PAN	— peroxyacetyl nitrate
THC	— total hydrocarbons

k_1	first-order dissociation constant for NO_2
$[OH]_{ss}$	steady-state hydroxyl radical concentration

ACKNOWLEDGMENTS

The authors especially thank Dr. T. A. Walter for his helpful discussions of reaction mechanisms and intermediates. We also thank Mr. T. Winfield (for assistance in analyzing for nitric acid), Mr. S. B. Joshi (for help in determining peroxyacetyl nitrate concentrations), and Mr. B. Gay and Dr. T. Knudsen (for aid in analysis of diethylhydroxylamine).

SECTION 1

INTRODUCTION

The idea of treating polluted air with a chemical "air freshener" has been bandied about in the literature for a number of years (1). The quest for a "suitable" free radical scavenger led Heicklen and others to suggest the use of DEHA as a photochemical smog inhibitor (2,3). Because of the announced intention of Heicklen and co-workers "to add DEHA into urban atmospheres to prevent the formation of photochemical smog" (4), and in an attempt to resolve the controversy (5,6) regarding the efficacy of DEHA in inhibiting the onset of the physical and chemical characteristics associated with smog formation, this study was undertaken.

SECTION 2

EXPERIMENTAL

A series of irradiation experiments was conducted in a smog chamber using propylene (C_3H_6) or n-butane (C_4H_{10}) as the HC. NO_x in the ratio 4 parts NO to 1 part NO_2 were added to the chamber, and DEHA was either introduced or excluded in order to ascertain what differences were attributable to the role of the inhibitor.

The irradiations were carried out in a 400-ft^3 smog chamber described elsewhere (7). A schematic diagram of the chamber and support equipment is shown in Figure 1. An average value for k_1 of 0.4 min^{-1} was measured.

Cylinders of NO in nitrogen (N_2) and NO_2 in N_2 from Scott Products® were used to charge the chamber with the initial NO_x concentrations. Propylene and n-butane used for these runs were supplied by Matheson Gas Products®. Anhydrous DEHA from Pennwalt Corporation® was used. Initially, DEHA was purified by vacuum distillation (4). However, this purification was discontinued for two reasons: (1) no difference in irradiations was attributable to use of the purified material; and (2) any widespread application of DEHA to smog control strategies would have to use unpurified commercial product.

NO and NO_x concentrations were monitored on two Bendix® chemiluminescent monitors. Periodic Saltzman determinations (8) of NO_2 concentration were made. O_3 was measured on a Bendix® Model 8002 O_3 monitor. HC concentrations were measured using an FID gas chromatograph (either a Perkin Elmer® Model 900 or a modified Beckman® 6800). Porapak® Q columns were used to separate and analyze the HC. DEHA in the gas phase was monitored using a Pennwalt® 223

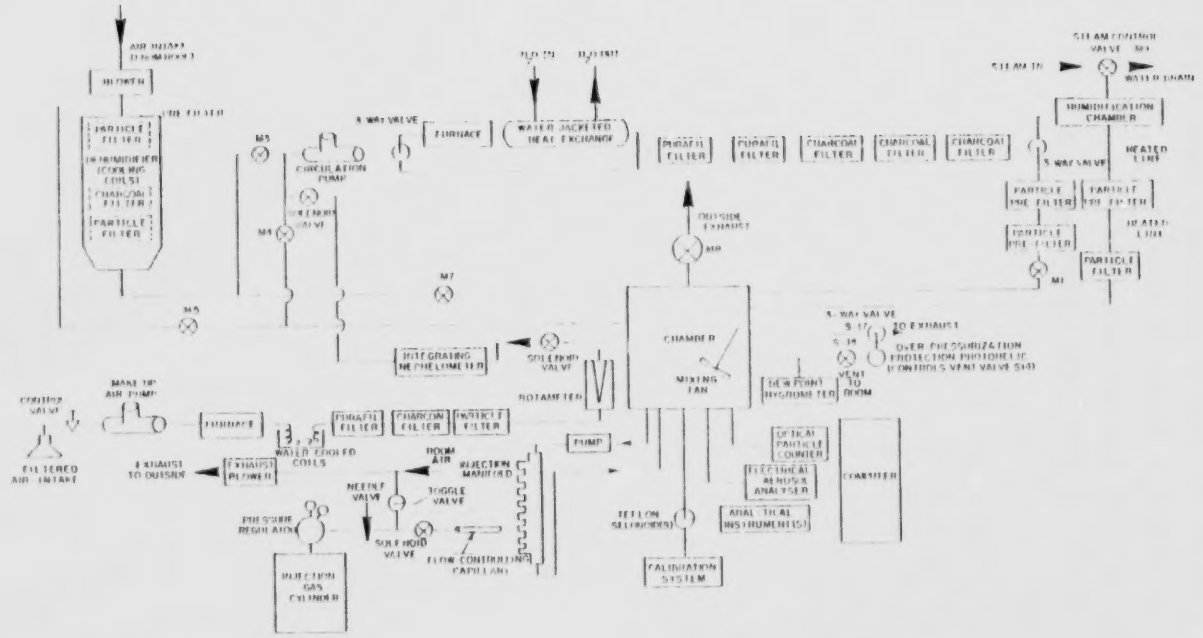

Figure 1. Schematic diagram of chamber and support equipment.

amine packing in either a glass or Teflon® column in the Perkin Elmer® Model 900 GC. Bag samples from the chamber were analyzed for peroxyacetyl nitrate (PAN) on the Perkin Elmer® GC with an electron capture detector. Aerosol formation was monitored with a Thermo Systems® EAA. The dew point for each run was held between 52-56°F and was monitored with an E G & G® dew point hygrometer. The internal chamber temperature was monitored with a YSI® calibrated thermistor.

SECTION 3

RESULTS

The reaction profiles for 47 HC/NO_x/DEHA runs are displayed in the Appendix. For convenience, selected runs will also be reproduced in the present section. For all of the runs reported here, the nominal initial concentrations of NO_2 and NO were 100 and 400 ppb, respectively. Stability measurements of DEHA and HC gave gas-phase loss rates in the nonirradiated chamber that were experimentally equivalent to the dilution losses.

Figure 2 shows the results of irradiating DEHA and NO_x, with no HC added. Conversion of NO to NO_2 was inhibited for about 6 hr, after which rapid conversion of NO and quick formation of O_3 occurred.

Figures 3 through 14 show the effects of irradiations with and without DEHA for a variety of HC concentrations. In Figures 3 and 4, the propylene concentration is ~0.25 ppm. In Figures 5 and 6, the propylene concentration is ~0.5 ppm, and in Figures 7 and 8 the HC concentration is ~5 ppm. Figures 9 through 14 show irradiations of n-butane. HC concentration in Figures 9 and 10 is ~0.5 ppm; in Figures 11 and 12, ~5 ppm; and in Figures 13 and 14, ~15 ppm.

These graphs of irradiation runs demonstrate strikingly the effects of DEHA on the system. During the initial portion of the run, the NO concentration increases as the NO_2 is converted to NO and atomic oxygen (O) by irradiation. HC consumption is decreased relative to the "no DEHA" profile, and O_3 formation is retarded. After the DEHA is consumed, the reaction proceeds with

vigor! The NO conversion is very rapid, O_3 formation is accelerated, and the maximum O_3 concentration attained is increased.

Table 1 shows data taken from propylene runs. The first column lists the Appendix figure number (e.g., "1" refers to Figure A-1). The second column gives the initial propylene concentration, the third column tabulates the initial DEHA concentration, and the fourth shows the ratio $[DEHA]_o/[HC]_o$. The next six columns represent various measurements of "smog formation." The time to reach 90% of initial NO concentration (i.e., 10% conversion to NO_2 and other products) is listed in minutes in column five. The time at which only 10% of $[NO]_o$ remains as NO is given in the next column. The times in minutes for O_3 to reach 40 ppb and to reach its maximum concentration are listed in the next two columns, while the maximum O_3 concentration obtained is given in column nine. The effective O_3 dosage for "1 day" (i.e., 11 hr of chamber irradiation) is given in the tenth column.

The next five columns list pseudo-first-order rate constants for HC or DEHA removal. (This assumes that concentrations of reactants other than HC or DEHA are unchanging; i.e., that steady-state approximations are valid for those species which react to remove the HC or DEHA.) The first two of these columns apply only to irradiations to which no DEHA has been added. The first column shows the rate constant calculated from data early in the reaction (i.e., prior to a substantial O_3 buildup), while the second column lists the overall removal rate constant. The third column tabulates the HC removal rate when DEHA was present, and the fourth gives the HC reroval rate after the DEHA has been consumed. Finally, the pseudo-first-order removal rate constant for DEHA plus hydroxyl (OH) is estimated.

Figures 15 through 17 plot some of the data on "smog formation" listed in Table 1 for the initial propylene concentrations of ~0.25, ~0.5, and ~5 ppm, respectively. Figure 15 demonstrates some interesting results. At $[DEHA]_o/[HC]_o = 0.2$, the initial conversion of NO to NO_x is retarded; once the reaction begins, however, the 90% conversion point (the + in the plot) is soon reached and is achieved earlier than in the no-DEHA case. Therefore, under these experimental conditions "smog formation" can be either retarded or enhanced,

depending upon which characteristic one chooses to examine. Note also that, while the onset of O_3 production may be retarded, it is entirely possible that the "1-day" O_3 dosage may be enhanced. Comparison of Figure 15 with Table 1 shows that, while the "1-day" O_3 dosage is reduced at high DEHA-to-HC ratios, it comes about not because the potential for large values of $[O_3]_{max}$ is reduced, but rather because the onset of O_3 formation is delayed sufficiently long for the integrated O_3-time profile for the first 11 hr of irradiation to be diminished.

Figures 5 and 6 demonstrate that PAN production seems to be increased when DEHA is added to the system. Also, Figure 8 includes the profile of HNO_3 formation as monitored by the method of Miller and Spicer (9).

Aerosol formation was monitored in a series of runs using the TSI® Model 3030 EAA. Figure 18 compares the aerosol data for some 5 ppm propylene runs, with and without DEHA.

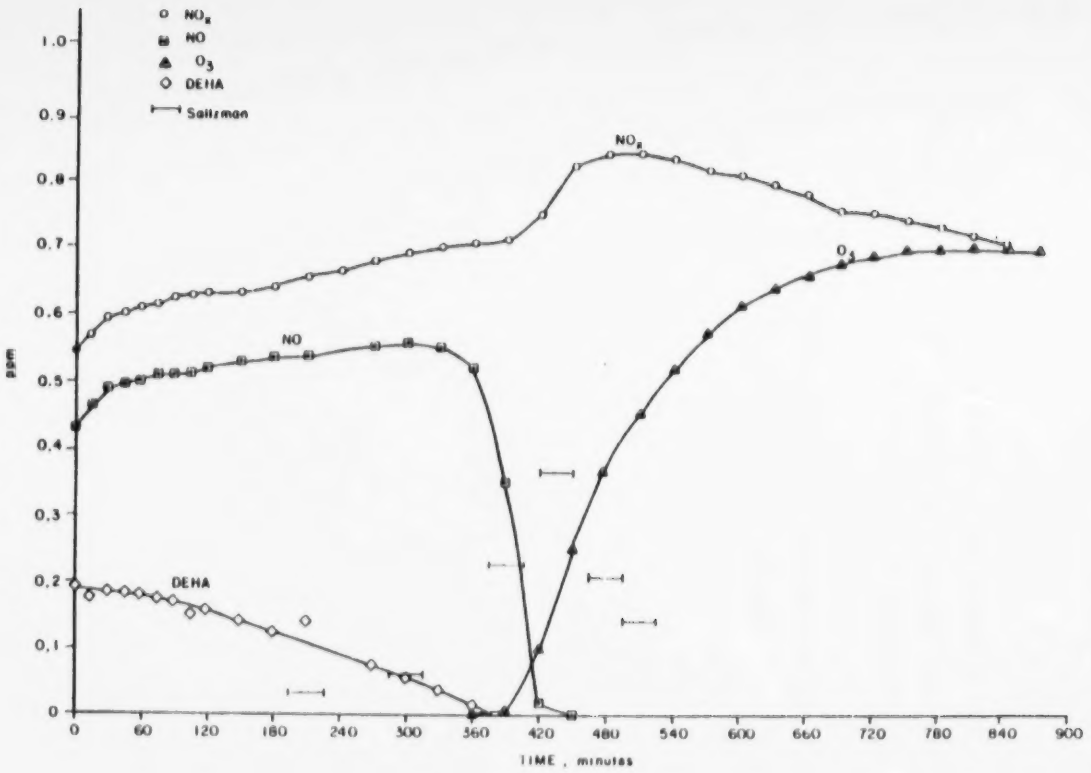

Figure 2. Reaction profiles of DEHA-NO_x system.

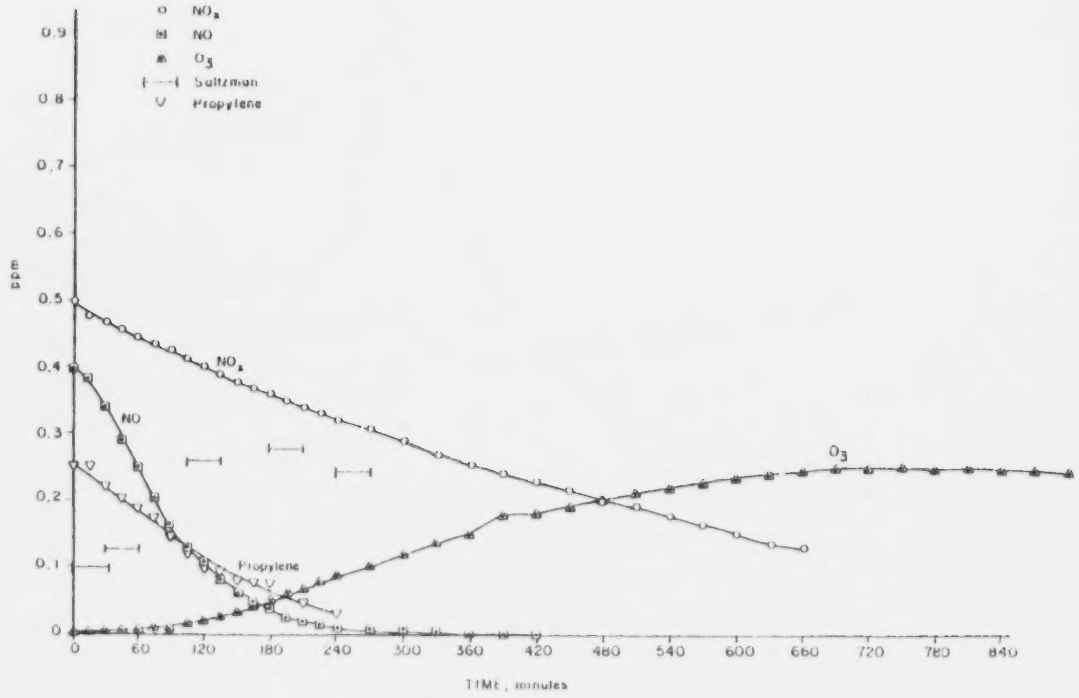

Figure 3. Reaction profiles of 0.25 ppm propylene-NO_x system.

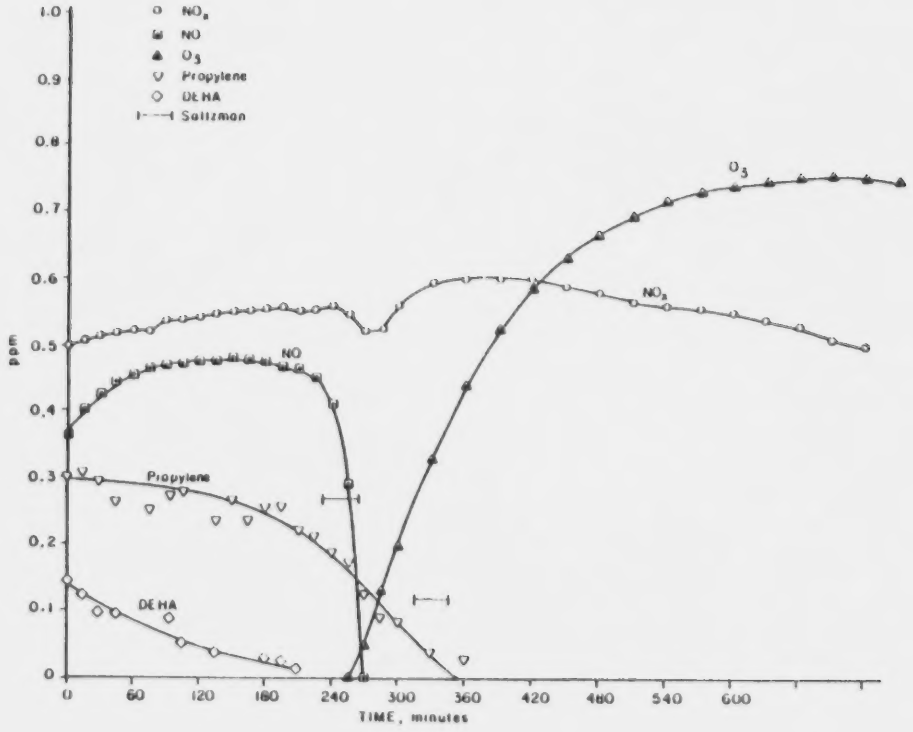

Figure 4. Reaction profiles of ~0.25 ppm propylene-NO_x-DEHA system.

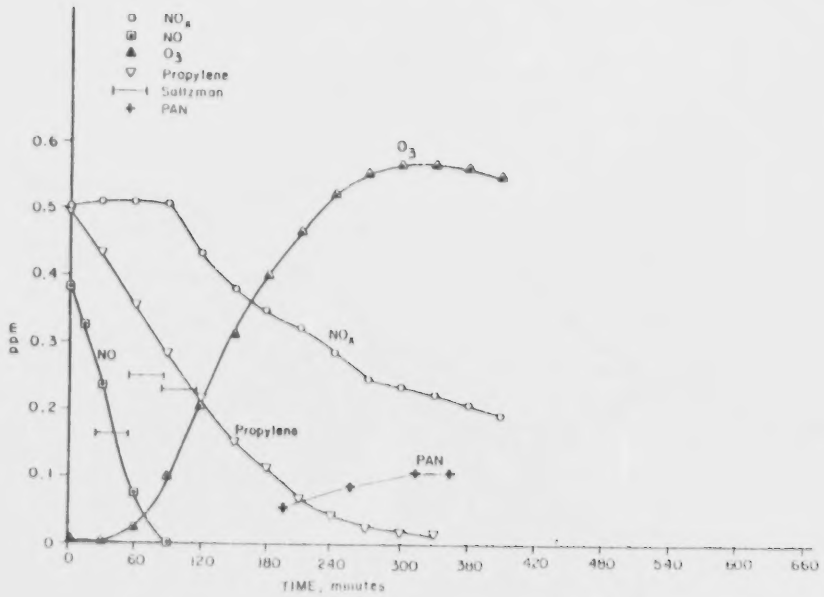

Figure 5. Reaction profiles of 0.5 ppm propylene-NO_x system.

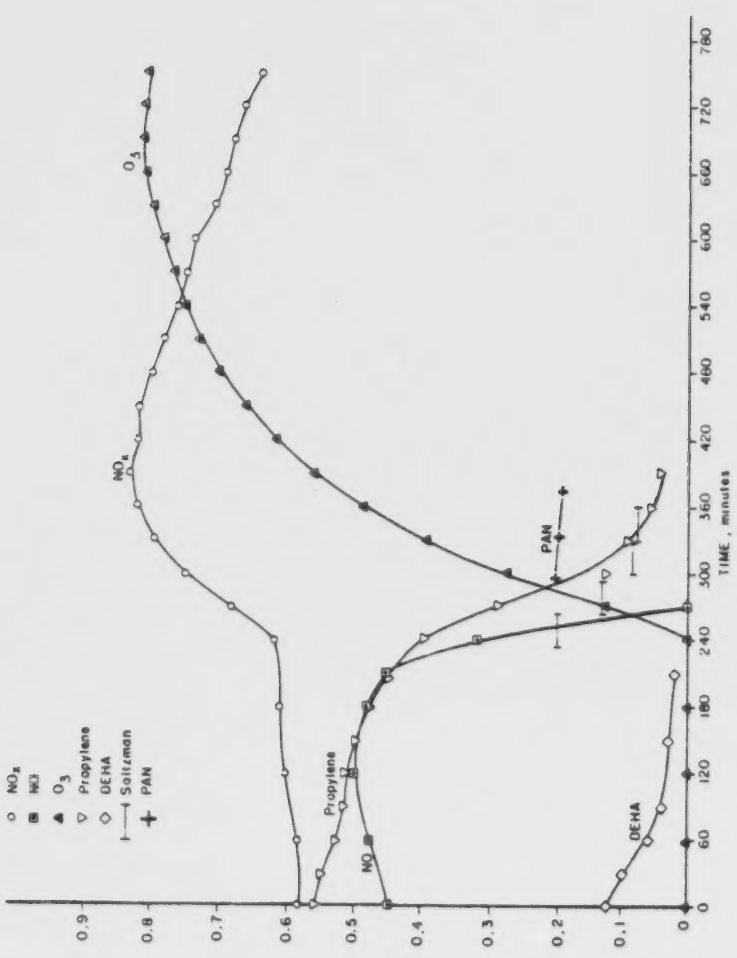

Figure 6. Reaction profiles of ~0.5 ppm propylene-NO_x-DEHA system.

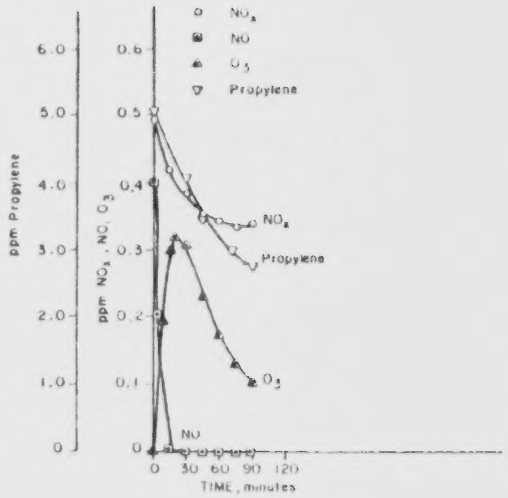

Figure 7. Reaction profiles of 5.0 ppm propylene-NO_x system.

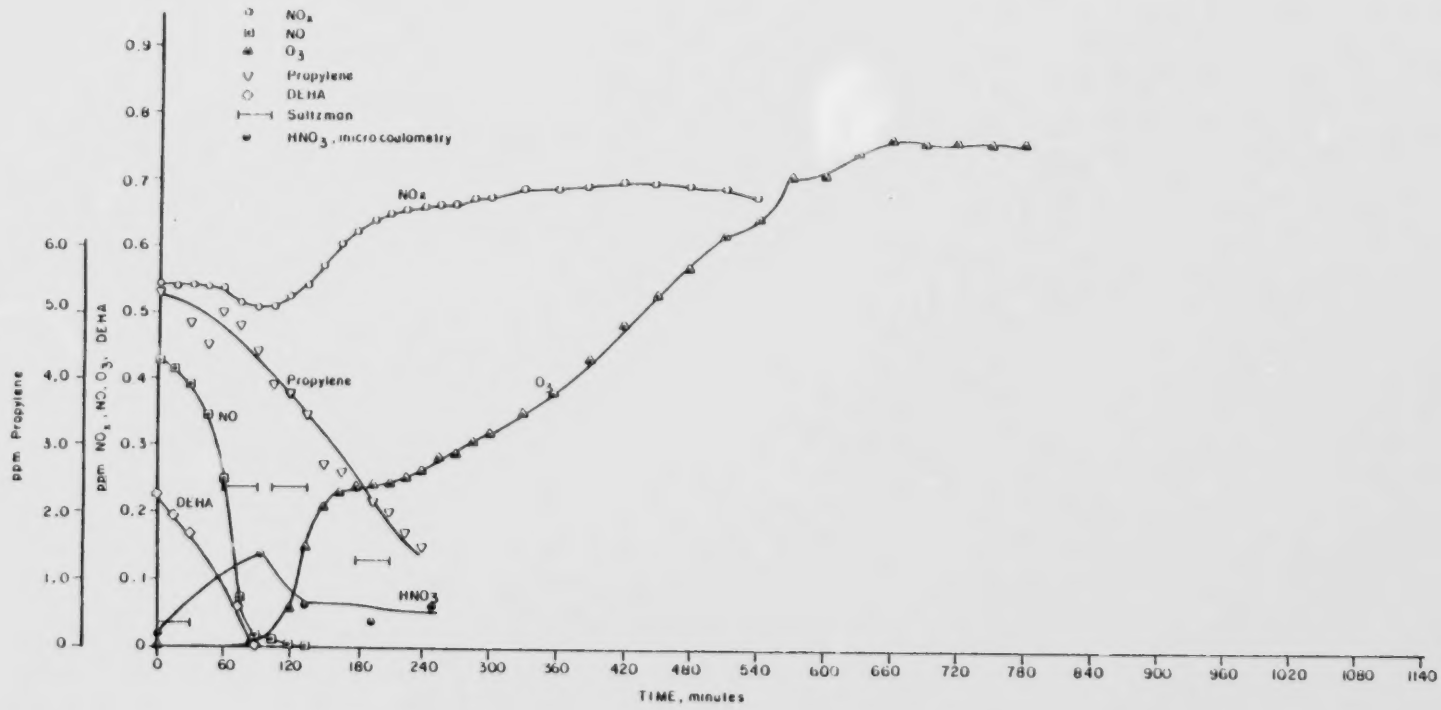

Figure 8. Reaction profiles of ~5 ppm propylene-NO_x-DEHA system.

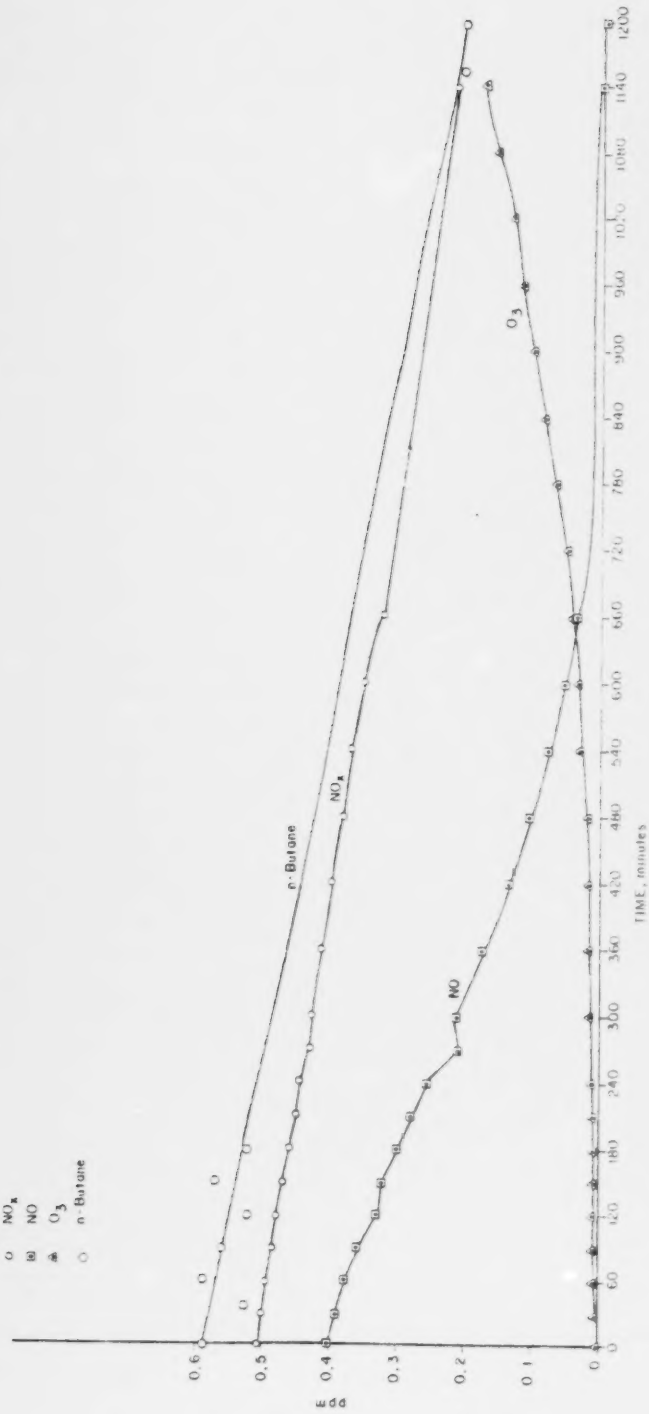

Figure 9. Reaction profiles of ~0.5 ppm n-butane-NO_x system.

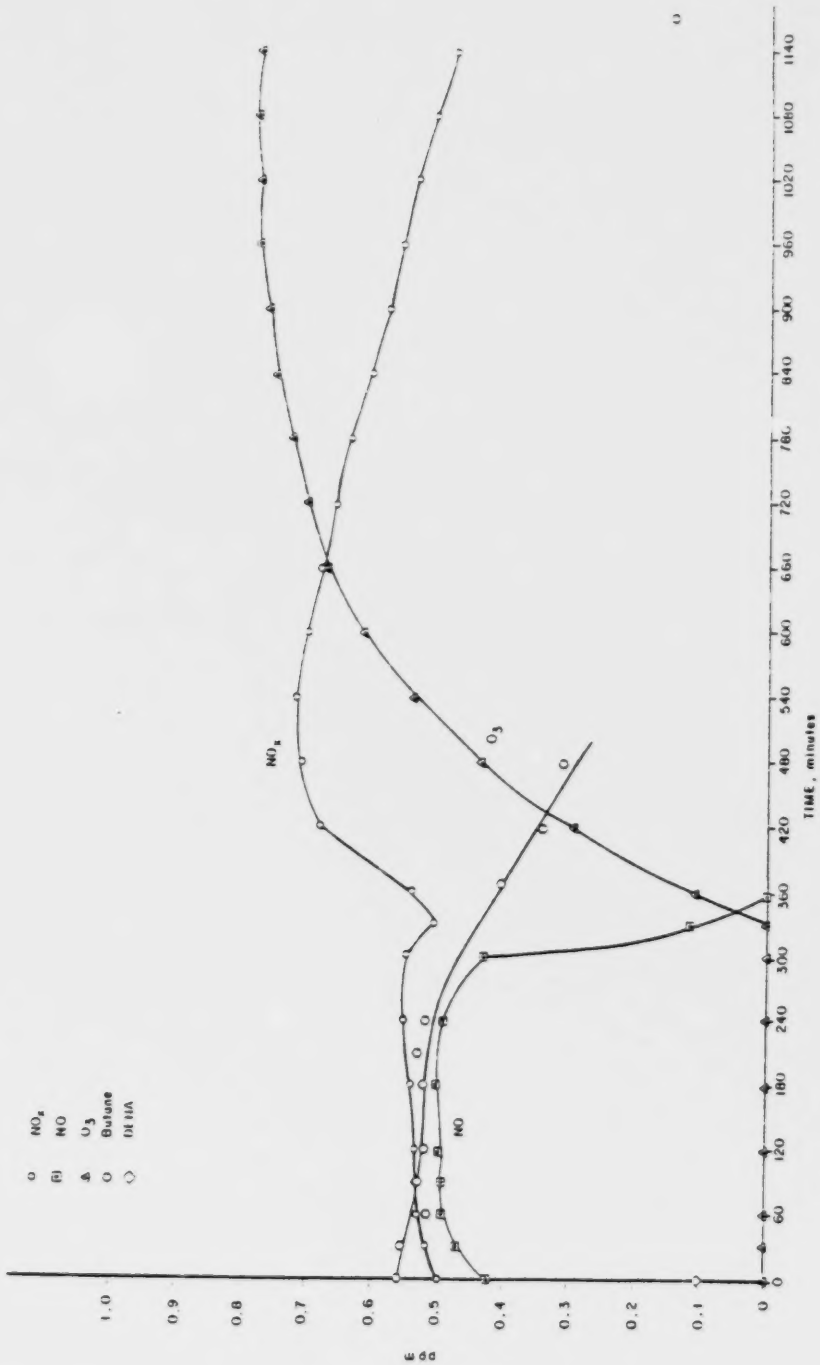

Figure 10. Reaction profiles of ~0.5 ppm n-butane-NO_x-DEHA system.

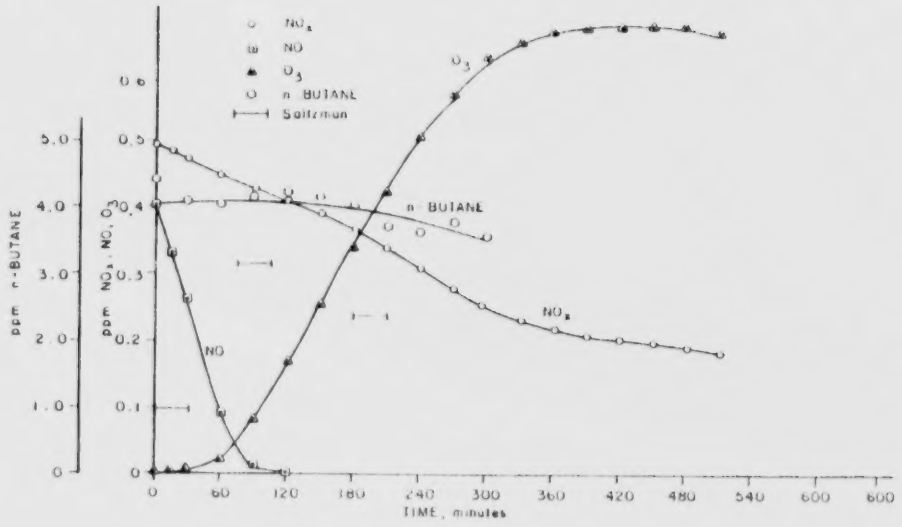

Figure 11. Reaction profiles of 5.0 ppm n-butane-NO_x system.

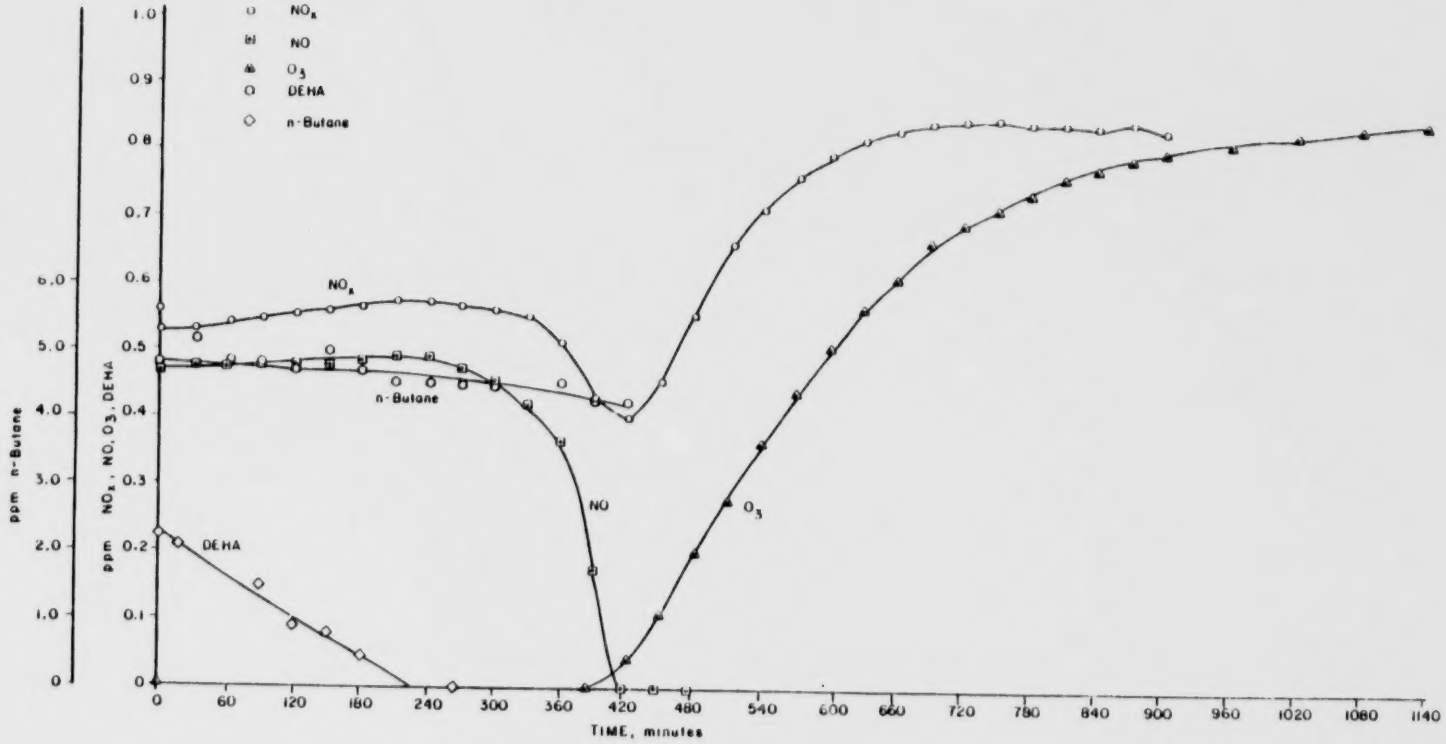

Figure 12. Reaction profiles of ~5 ppm n-butane-NO_x-DEHA system.

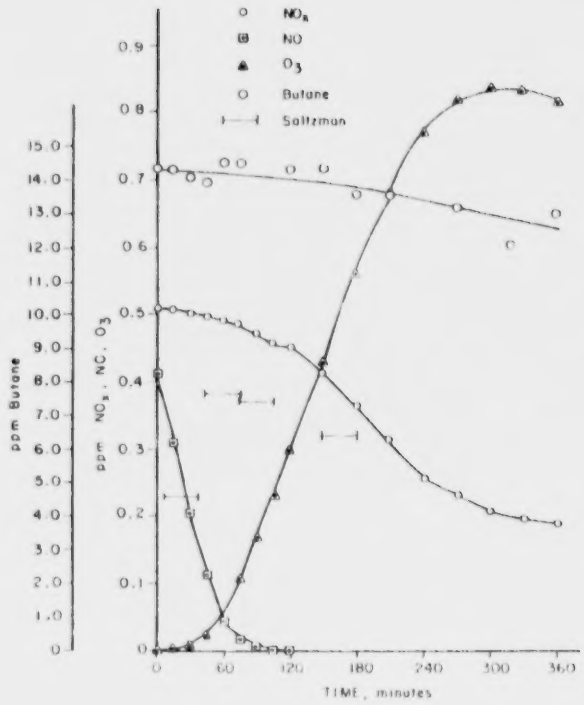

Figure 13. Reaction profiles of ~15 ppm n-butane-NO_x system.

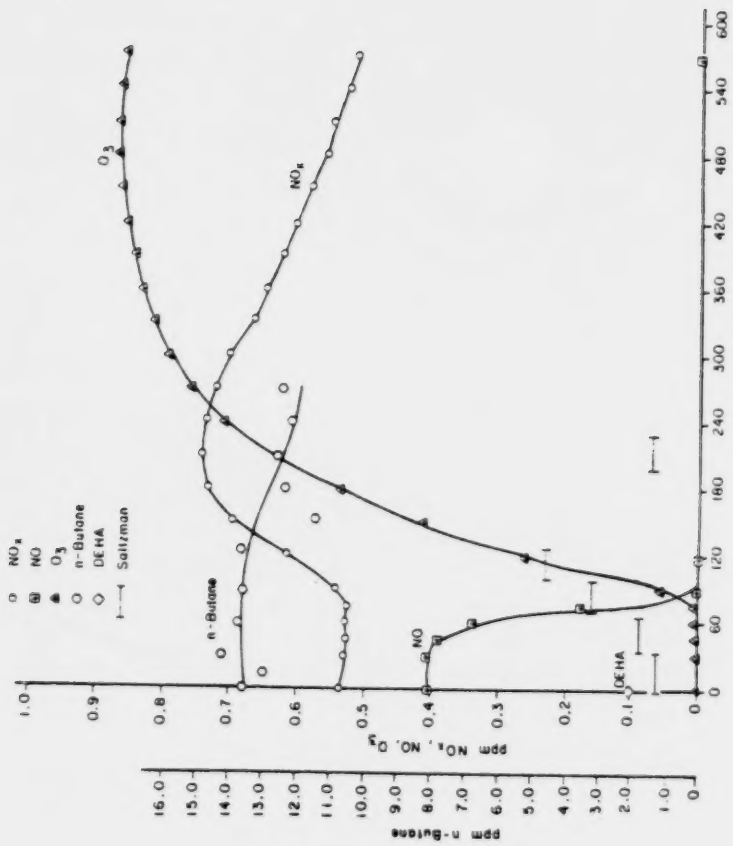

Figure 14. Reaction profiles of 15.0 ppm n-butane-NO_x-DEHA system.

TABLE 1. RESULTS OF IRRADIATION OF HC/NO_x/DEHA MIXTURE USING PROPYLENE

Figure	$[HC]_0$ ppmC	$[DEHA]_0$ ppb	$\frac{[DEHA]_0}{[HC]_0}$	TIME FOR $0.9[NO]_0$ min	TIME FOR $0.1[DEHA]_0$ min	TIME FOR Ozone = 40 ppb min	$[O_3]_{max}$ min	$[O_3]_{max}$ ppb	"ONE DAY" O_3 DOSAGE ppb-min	k_{HC} Removal: Ozone ≤70 ppb min^{-1}	k_{HC} Removal: Overall min^{-1}	k_{DEHA}: DEHA Present min^{-1}	k_{DEHA}: DEHA Consumed min^{-1}	k_{DEHA} min^{-1}	$k_{DEHA+OH}$ 10^5 ppm^{-1} min^{-1}
1	0.0	0.19	--	380	418	400	840	700	117	--	--	--	--	--	--
2	0.25	0.00	0.00	25	165	165	750	230	85	.00655	.00655	--	--	--	--
3	0.25	0.00	0.00	25	171	165	780	260	82	.00550	.00550	--	--	--	--
4	0.24	0.05	0.21	46	83	75	480	540	243	--	--	.00513	.02463	.04748	3.3
5	0.26	0.10	0.38	274	288	288	900	800	194	--	--	.00134	.02267	.01008	2.7
6	0.30	0.15	0.50	253	268	266	660	750	223	--	--	.00151	.01337	.01103	2.6
7	0.30	0.38	1.27	474	495	495	930	900	60	--	--	.00072	--	.00453	2.3
10	0.50	0.00	0.00	14	93	81	430	525	241	.00564	.00700	--	--	--	--
13	0.54	0.00	0.00	8	60	55	405	470	236	.00853	.01006	--	--	--	--
21	0.52	0.00	0.00	8	77	64	360	590	294	.00735	.00900	--	--	--	--
22	0.50	0.00	0.00	11	67	67	340	570	279	.00501	.00842	--	--	--	--
11	0.60	0.13	0.21	191	208	204	*	*	*	--	--	.00255	.02472	.00957	1.4
23	0.55	0.13	0.23	226	267	252	715	810	240	--	--	.00094	.02041	.00669	2.6
12	0.50	0.13	0.25	168	194	189	510	700	253	--	--	.00024	.03047	.00946	14.2
15	0.50	0.15	0.30	215	237	234	600	630	213	--	--	.00102	.02387	.00871	3.3
25	5.2	0.00	0.00	2	9	8	23	330	22	--	.00763	--	--	--	--
26	5.3	0.00	0.00	1	9	7	20	320	23	--	.00749	--	--	--	--
27	5.3	0.23	0.04	45	80	115	750	760	245	--	--	.00239	.00773	.01037	1.6
28	4.7	0.28	0.06	42	85	125	840	760	255	--	--	.00073	.00822	.01163	8.7
29	4.9	0.50	0.10	85	132	180	840	740	183	--	--	.00114	.00555	.00947	3.0
30	5.0	0.76	0.15	175	245	300	990	700	98	--	--	.00026	.00545	.00446	6.2
31	4.7	1.4	0.30	310	353	402	1150	800	65	--	--	.00071	.00298	.00931	4.7

*Equipment Failure During Run

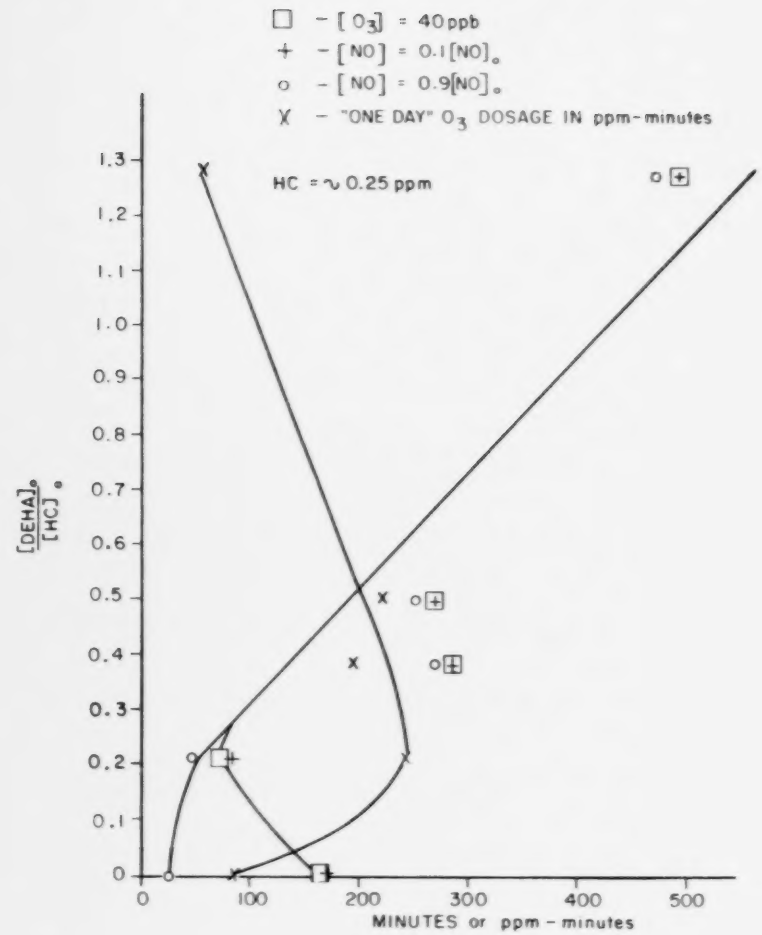

Figure 15. Effect of changes of $[DEHA]_o/[HC]_o$ on manifestations of "smog" for an initial HC concentration of ~0.25 ppm propylene.

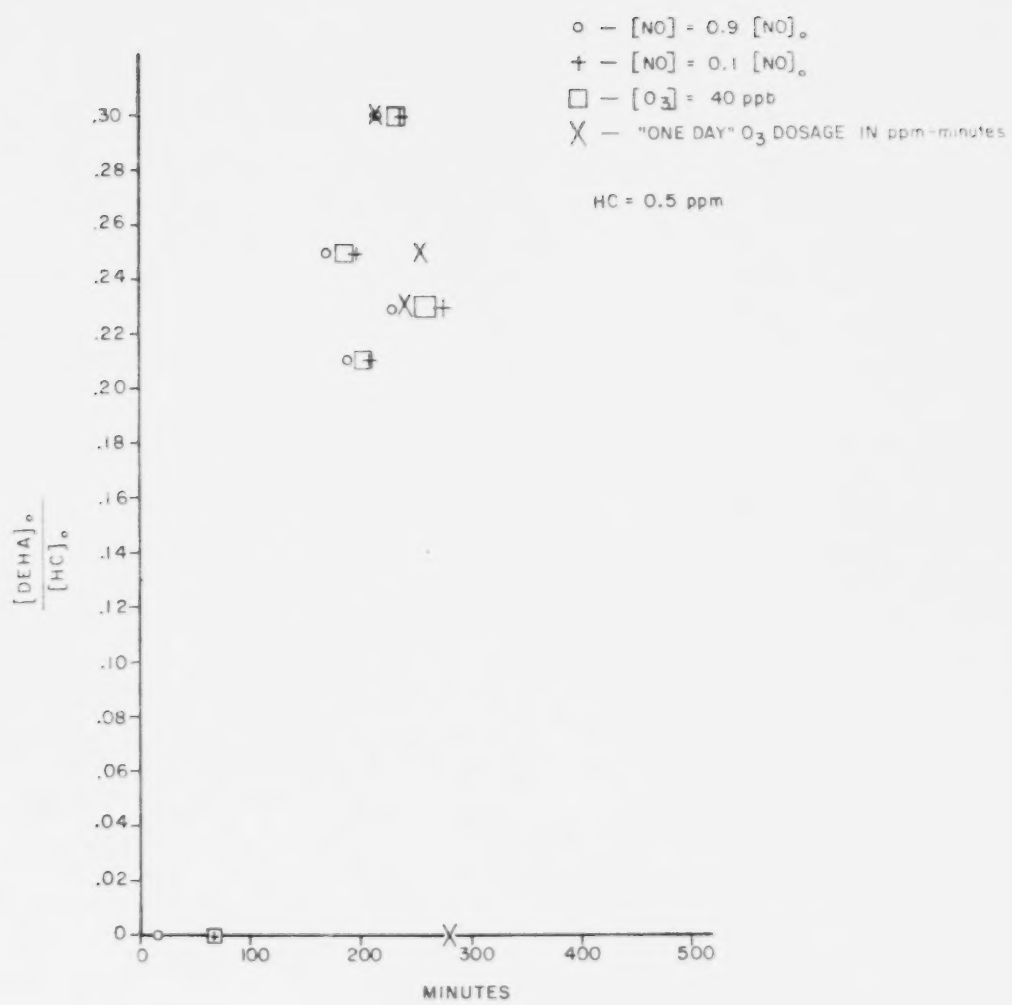

Figure 16. "Smog" manifestations for an initial HC concentration of ~0.5 ppm propylene.

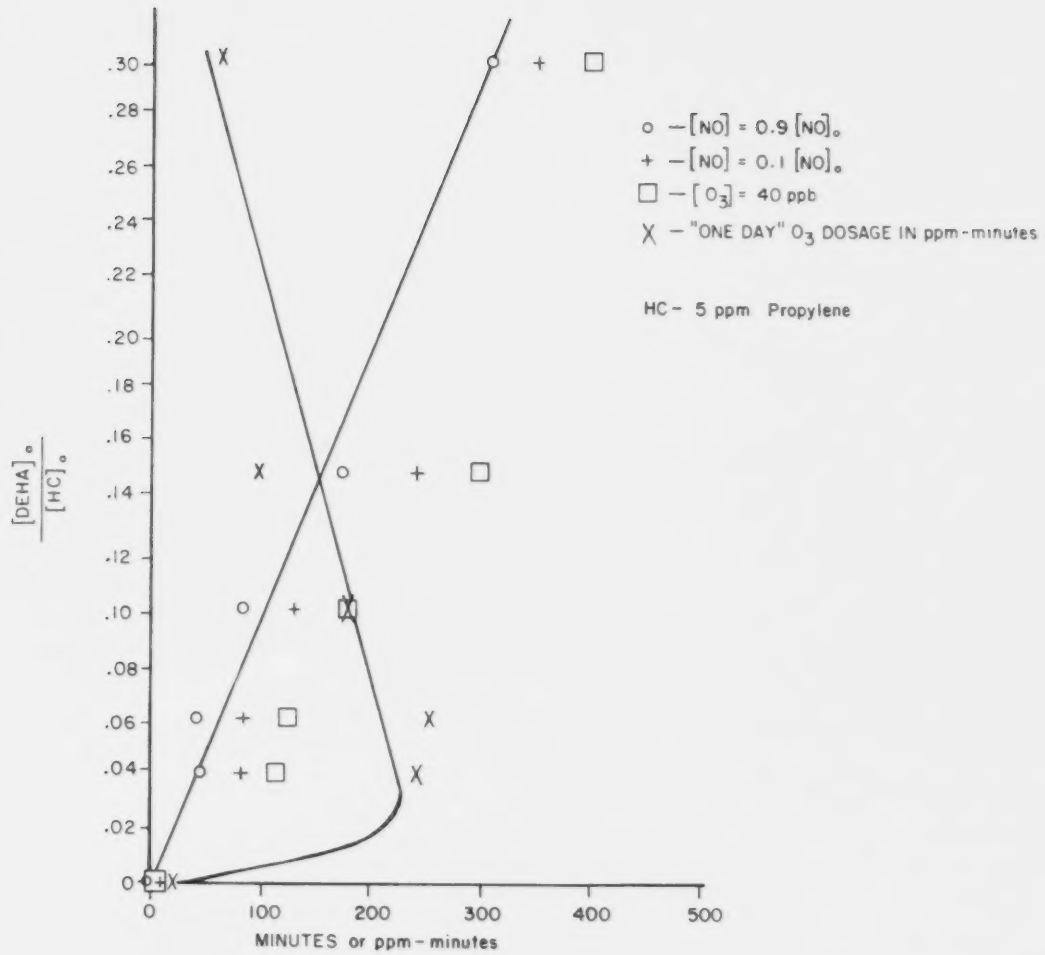

Figure 17. Effect of $[DEHA]_o/[HC]_o$ on "smog" manifestations for an initial HC concentration of ~5 ppm propylene.

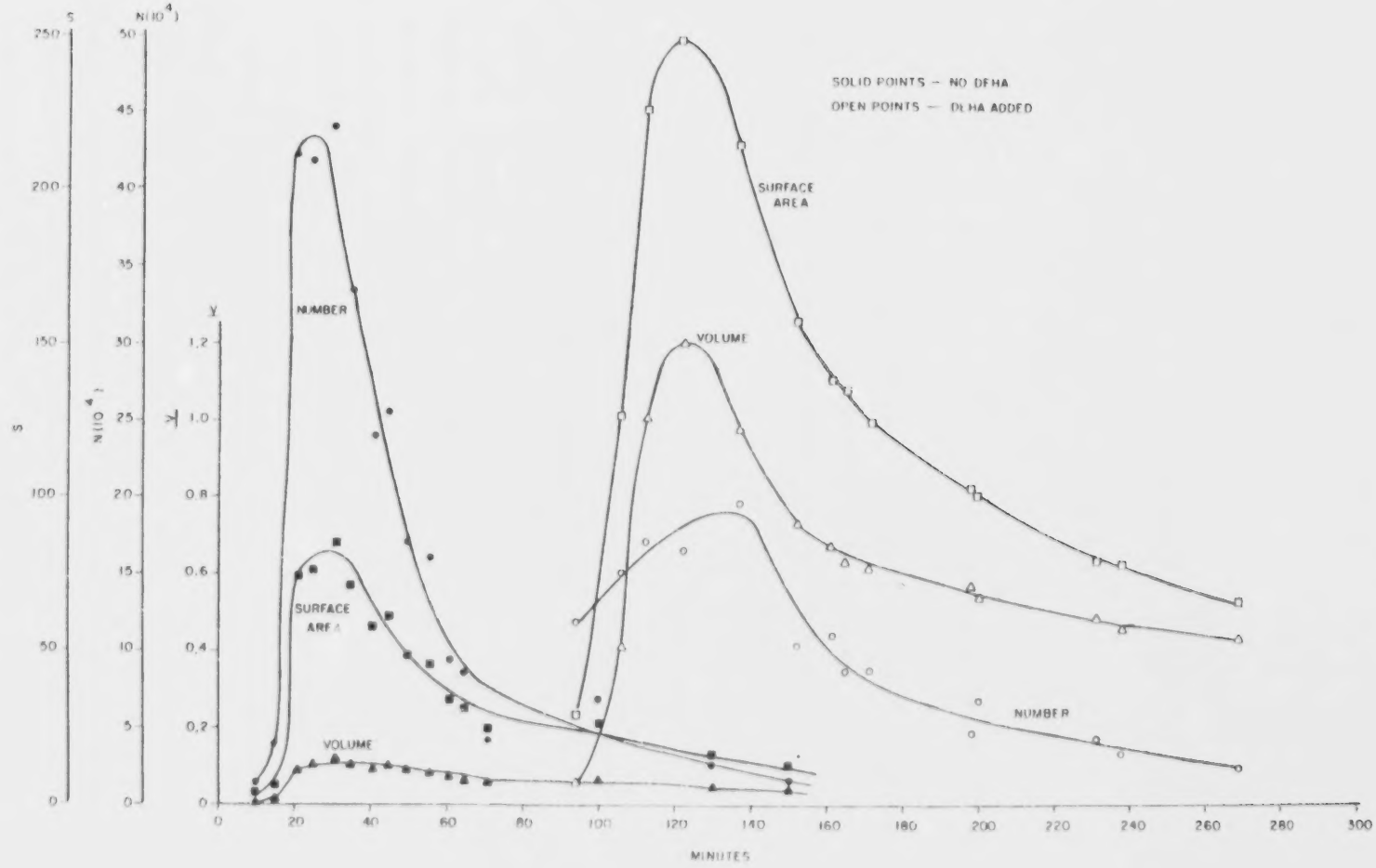

Figure 18. Aerosol formation data versus time for runs with (open symbols) and without (filled symbols) DEHA.

SECTION 4

DISCUSSION

DEHA EFFECTS ON ASPECTS OF SMOG FORMATION

The results reported above illustrate that DEHA does indeed exhibit remarkable influence on the progress of smog formation in chamber irradiations. The effect of DEHA on a number of characteristics normally attributed to smog formation will be discussed below.

NO Conversion

One of the earliest suggestions for using DEHA as an inhibiting agent arose because of its ability to inhibit conversion of NO to NO_2 (2). A series of 10-min irradiations of $NO/C_3H_6/O_2$ were carried out, and the amount of NO_2 formed was monitored. DEHA was found to be one of the more efficient compounds for retarding the formation of NO_2. The data presented herein confirm that result: DEHA does inhibit the conversion of NO to NO_x products. Indeed, in this system, NO_2 initially decreases while NO increases. But 10-min irradiations do not tell the whole story, for — in all but the most reactive HC/NO_x systems — the addition of DEHA first inhibits and then accelerates the conversion of NO. As can be seen from Table 1, experimental conditions can be found for which conversion of the first 10% of NO is retarded while conversion of 90% of the NO is accelerated. (See also Figures 9 and 10 for the 0.5 ppm n-butane runs and Figures 11 and 12 for the 15 ppm n-butane runs, where the DEHA-added runs exhibit similar behavior.) This means that the effect of DEHA in inhibiting NO conversion to products is ambiguous, and that short irradiation experiments could show an inhibiting effect, while longer irradiations would indicate an enhancement.

O_3 Formation

The data in Table 1 and the reaction profiles in the Appendix all show $[O_3]_{max}$ to be increased by the addition of DEHA to the reaction system. With DEHA added to the propylene system, $[O_3]_{max}$ ≈750 ppb. This compares to ~250 ppb, ~550 ppb, and ~330 ppb for the 0.25 ppm, 0.5 ppm, and 5.0 ppm propylene runs, respectively.

In fairly reactive systems, the onset of O_3 production (as represented by the time at which the O_3 concentration reaches 40 ppb) and the time for O_3 maximum are retarded by DEHA. However, in the case illustrated by Figure A-4, both onset of O_3 formation and the time for $[O_3]_{max}$ are advanced by the addition of DEHA. Coupled with an increased value for the O_3 maximum, the "1-day" O_3 dosage is three times as large with 50 ppb of DEHA in the system as with no DEHA.

O_3 dosages were determined by measuring the area under the O_3 concentration profile for the first 11 hr of irradiation. Schere and Demerjian (10) give 1/2-hr average values of k_1 for June 21 in Los Angeles. In our experiments, the area under the sinusoidal-like step function was calculated to give a k_1·time product. The result was divided by the chamber k_1 value of 0.4 to determine the length of time of chamber irradiation equivalent to the Schere and Demerjian k_1 profile. This time was reduced by about 10% to represent the solar irradiance on an average spring or summer day instead of for the longest day of the year. (Data taken from Leighton (11) for a point at 35°N latitude indicate that daily insolation for an average spring and summer day is about 89% of the daily insolation at summer solstice.) The result was that an 11-hr irradiation in the chamber gave a k_1·time product equivalent to that of an average spring/summer day in Los Angeles; the integrated dosages for 11-hr irradiations are given in Table 1 and Figures 15 through 17.

In general, the time for onset of O_3 production and the time to reach O_3 maximum increase with increasing DEHA concentration. This affects the "1-day" dosage figures, not by reducing the O_3-forming potential of the system but

rather by moving the O_3 profile out of the first 11-hr irradiation period. Even so, the dosage figures are not lowered relative to the no-DEHA case until a substantial amount of DEHA has been added.

PAN Formation

The addition of DEHA to the propylene-NO_x system roughly doubles the maximum PAN concentration reached during irradiation (cf. Figures 5 and 6). A similar result is reported by Pitts *et al.* (5).

Aerosol Formation

Figure 18 compares the aerosol growth dynamics of chamber irradiations with and without DEHA. In both instances, the rapid production of aerosol coincides with the onset of O_3 formation. Without DEHA, a large number of small droplets is formed. With DEHA in the system, the number of particles formed is not so large as in the "no-DEHA" case, but they are larger in diameter (as evident in the substantial increases in volume and surface area). This means that there is considerably more material tied up in the aerosol when DEHA is in the system. Also, only with DEHA added do the aerosol particles exceed 0.05 μm in diameter. Since 0.05 μm is (roughly) the smallest size particle that can contribute to particulate light scattering (12), the net effect of DEHA on visibility would seem to be increased degradation resulting from particulate diffusion.

HC Consumption

A second major inhibiting characteristic (in addition to retarding NO conversion) ascribed to DEHA is that it slows the rate of HC consumption (4,6). This is to be expected of any compound which can effectively compete with the HC for those reactive species which are capable of removing the HC. Because the predominant reactive species early in an irradiation is OH (12), any compound which reacts with OH at a rate substantially higher than that of the HC should effect a decrease in the HC consumption rate — so long as its reaction products do not in turn produce even more OH or other reactive species.

Table 1 shows that DEHA does substantially reduce the HC consumption rate as long as DEHA is present in the chamber. Once all the DEHA has been consumed, however, the HC removal rate is accelerated and becomes as fast or faster than the removal rate in the "no-DEHA" case.

Figures 9 through 14 demonstrate a similar general behavior for n-butane (i.e., the HC removal rate is decreased as long as DEHA is present and is increased after all the DEHA has been consumed).

The data listed in Table 1 for $K_{HC\ Removal}$ permit some interesting calculations. If one assumes that HC removal prior to substantial buildup of O_3 is primarily due to reaction with OH (12), then the steady-state hydroxyl radical concentration $[OH]_{ss}$ can be estimated as

$$[OH]_{ss} = (k_{HC\ Removal} - k_{Dilution})/k_{HC+OH}$$

Using the data for $k_{HC\ Removal}$ (with $O_3 \leq 70$ ppb) together with values of 2.6×10^{-4} min^{-1} and 3.6×10^{4} ppm^{-1} min^{-1} for $k_{Dilution}$ and k_{HC+OH} (13), one calculates an average OH concentration of 1.6×10^{-7} ppm, or about 4×10^{6} radicals cm^{-3}. This value is roughly equivalent to the yearly daytime average [OH] of 5×10^{6} radicals cm^{-3} calculated by Weinstock (14), and is less than the daytime OH concentrations in ambient air measured by Niki *et al.* (15).

The validity of using HC removal rate data taken before $[O_3]$ reaches 70 ppb can be checked by calculating the ratio of HC removed by OH to the HC removed by O_3:

$$R = \frac{k_{HC+OH}\ [OH]_{ss}[HC]}{k_{HC+O_3}\ [O_3]\ [HC]}$$

For the propylene data given in Table 1, the ratio is:

$$R = \frac{(3.8 \times 10^{4}\ ppm^{-1}\ min^{-1})\ (1.6 \times 10^{-7}\ ppm)}{(1.7 \times 10^{-2}\ ppm^{-1}\ min^{-1})\ (0.070\ ppm)} \approx 5.1$$

This means that the HC removal rate is dominated (by a ratio of 5:1 or greater) by the OH reaction until O_3 exceeds 70 ppb. This calculation neglects HC removal by other species like hydroperoxide (HO_2) and O, the concentrations of which are kept exceedingly low by other species present in the system.

One may assume that when both DEHA and propylene are present in the chamber they compete for the same reactive species. If that species is OH, then one may estimate the reaction rate constant for DEHA plus OH by the following equation:

$$k_{\text{DEHA + OH}} = \frac{k_{\text{DEHA Removal}} \cdot k_{\text{HC + OH}}}{k_{\text{HC Removal (DEHA Present)}}}$$

The last column in Table 1 shows the estimated values for DEHA + OH determined from the experimental runs. The results give a value of 4.1×10^5 ($\pm 3.4 \times 10^5$) $ppm^{-1}\ min^{-1}$. This value is in good agreement with the direct measurement of 1.4×10^5 $ppm^{-1}\ min^{-1}$ reported by Gorse *et al.* (16), especially in view of the assumptions required to obtain the estimate. This value is approximately one-half the "hard-sphere" estimate for a collisional rate constant and implies that the reaction of DEHA with OH is very efficient.

The data show that the parent compound DEHA can act to inhibit many of the manifestations of smog formation. However, as Figure 2 illustrates, DEHA is an organic molecule which, when irradiated with NO_x, yields reactive products. These primary or secondary products may, in turn, rapidly convert NO to NO_2 and form copious quantities of O_3. This implies that the "reactivity" of DEHA itself may set the limit on the extent of inhibition which is attainable by injection of DEHA into the atmosphere. Indeed, the striking similarity of Figure 2 (DEHA alone) and Figure 10 (DEHA added to 0.5 ppm n-butane) supports the idea that, in reasonably unreactive systems, smog formation is directly controlled by the reactivity of the DEHA itself.

POTENTIAL MECHANISMS TO EXPLAIN DEHA EFFECTS ON SMOG FORMATION

The behavior of the chamber runs described above can be explained in general terms by assuming that DEHA interacts with OH and other reactive intermediates to form inert or less reactive products. (Indeed, the primary applications for DEHA suggested by the manufacturer, Pennwalt, are as a radical scavenger or "shortstopper" in polymerization or corrosion chemistry (17).) Radical scavenging by DEHA would: (1) reduce the number of radicals capable of reacting with HC, thus reducing the HC removal rate; and (2) intercept atomic O so that irradiation would convert the NO_2 to NO with subsequent suppression of O_3 formation.

Attempts were made to adapt a reaction model for a propylene-NO_x system developed by Dodge and Ascher (private communication) to explain the results described above. Reactions for DEHA were added to the mechanism, based upon reported product formation.

The products attributed by Heicklen (4) to addition of DEHA to a $C_2H_4/NO/O_2$ irradiation system are: acetaldehyde (CH_3CHO) (C_2H_4O) (ALD2), ethyl nitrite ($C_2H_5NO_2$) (NET), ethyl nitrate ($C_2H_5ONO_2$) (NIT), ethanol (C_2H_5OH), nitrous acid (HONO), and nitrous oxide (N_2O) (N20). The reaction of O_3 with DEHA (in the presence of excess O_3 or air) is reported to yield CH_3CHO and $C_2H_5NO_2$ essentially quantitatively and without inhibition (18).

One possible mechanism that explains all of the observed products is shown in Figure 19. The first reaction step, abstraction of the hydroxyl hydrogen, was suggested by Heicklen (4) and supported by Gorse *et al.* (16), based upon liquid phase kinetic studies. Abstraction reactions are often very fast; in the case of abstraction by OH, a very stable product, water (H_2O), is formed. The resulting radical, $(C_2H_5)_2$-N-O· or DENO, is interesting in that resonant configurations may place the free electron on either the O or N atom. The intermediate DENO or some subsequent product may itself be relatively unreactive, since the rapid conversion of NO (and the other manifestations of smog formation) is suppressed so long as DEHA is still present in the chamber.

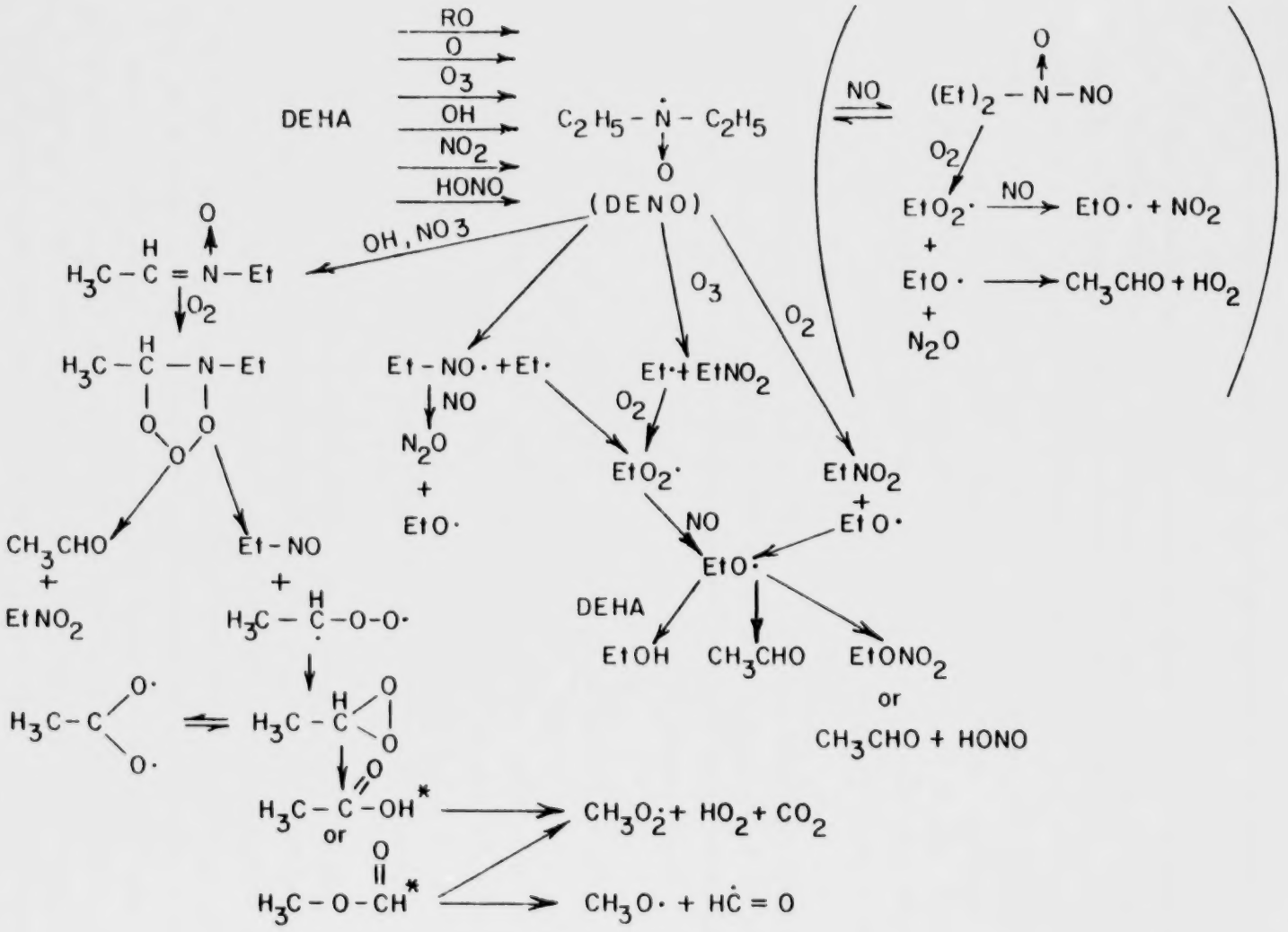

Figure 19. Possible reaction mechanism for DEHA.

Heicklen (4) reported an ~40-min inhibition period between onset of DEHA removal and the appearance of CH_3CHO, nitroethane ($CH_3CH_2NO_2$) ($EtNO_2$) and N_2O. He suggests that the compound $(Et)_2\overset{\oplus}{N}\overset{\ominus}{O}$-NO may serve as an unidentified intermediate in the reaction scheme. (The suggested reactions are included in parentheses in Figure 19.) Some of the reactions included in the mechanism must be considered to be speculative in nature. The paucity of thermodynamic data makes theoretical predictions of possible reaction routes and rates extremely difficult.

The photolytic rate constants in the model and an initial concentration of HONO were adjusted to emulate the NO removal rate observed in the chamber runs without DEHA. The model overpredicts O_3 formation (therefore, the HC removal rate is also too fast), a feature characteristic of this particular model (Dodge and Ascher, private communication). Reactions involving DEHA were then added to the mechanism. Initial attempts at modeling the entire reaction scheme actually increased the overall reaction rate. For simplicity, the DEHA reaction scheme was truncated with DENO, and the simulation was rerun in an attempt to model the initial portion of the irradiation. Figure 20 shows a comparison of the simulations with and without DEHA added.

The simulations show that, with this particular reaction mechanism, the addition of DEHA does indeed retard onset of O_3 production and NO conversion and slow the HC removal rate. The NO does increase initially, as is observed experimentally (although the model achieves this primarily through reaction of DEHA with HONO). The difficulties involved in modeling the initial NO increase indicate that the mechanism may be either incomplete or inadequate in regard to NO_x chemistry. This may also be the reason that the model tends to over-predict O_3 formation.

The rate constant used for Reaction (a)

$$\text{DEHA} + \text{OH} \rightarrow \text{DENO} + H_2O \qquad \text{(a)}$$

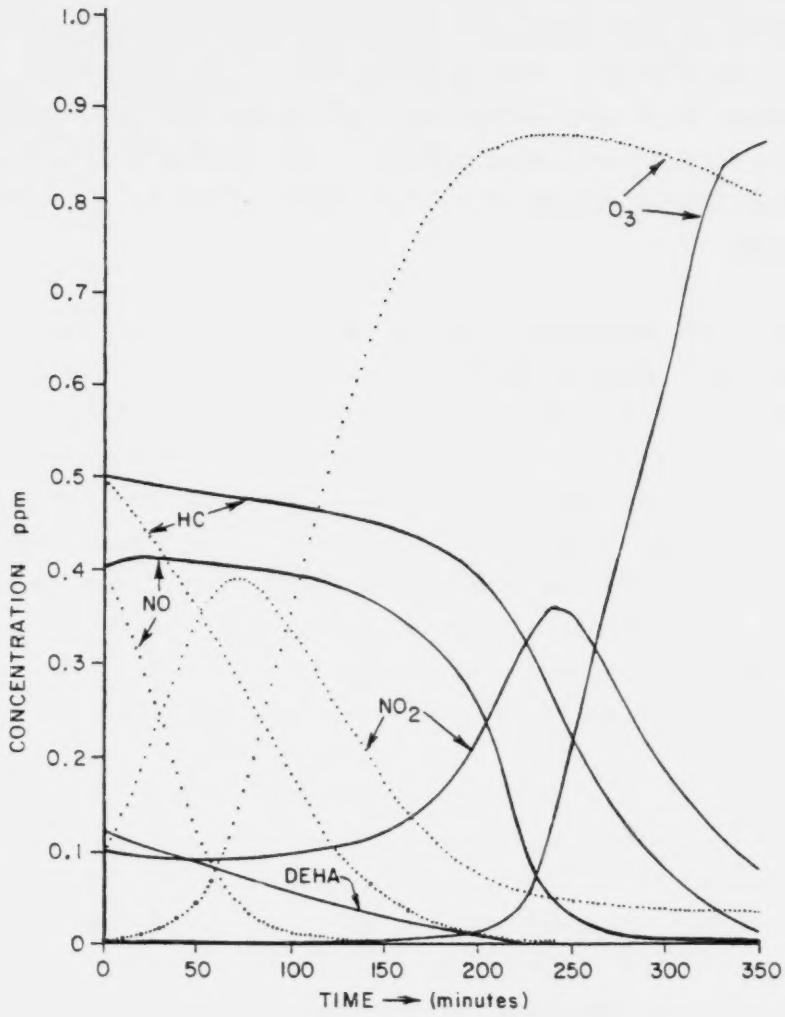

Figure 20. Simulation profiles for HC, NO, NO_2, O_3, and DEHA predicted by kinetic model. Initial concentrations are: $[HC]_o$ = 0.5 ppm propylene; $[NO]_o$ = 0.4 ppm; $[NO_2]$ = 0.1 ppm; $[O_3]_o$ = 0.0 ppm; and $[DEHA]_o$ = 0.0 or 0.125 ppm. Dotted lines are the "no DEHA" case. Solid lines show simulation with DEHA included.

varied between 1.4×10^5 ppm^{-1} min^{-1} and 4.1×10^5 ppm^{-1}, with an intermediate value of $\sim 2.6 \times 10^5$ ppm^{-1} min^{-1} generally being used.

An upper limit of 0.02 ppm^{-1} min^{-1} was estimated for reaction (b)

$$DEHA + NO_2 \rightarrow DENO + HONO \qquad (b)$$

based upon data obtained while charging the chamber for irradiations and from data quoted by Heicklen (2). B. Gay detected by Fourier transform infrared spectroscopy (FTIR) the rapid formation in the dark of HONO from the mixture of NO_2 and DEHA in a different chamber, but that rapid reaction may have been influenced by wall effects.*

The rate constant for reaction of O_3 and DEHA

$$O_3 + DEHA \rightarrow DENO + OH + O_2 \qquad (c)$$

was estimated as >1.3 ppm^{-1} min^{-1} from plots of the reaction of O_3 with DEHA published by Heicklen (18). A similar lower limit rate constant was used for reaction (d):

$$O + DEHA \rightarrow DENO + OH \qquad (d)$$

The reaction rate constant of HONO and DEHA was permitted to vary as required:

$$HONO + DEHA \rightarrow DENO + H_2O + NO \qquad (e)$$

Ratios of the subsequent reactions can be estimated from product distributions. The magnitudes of the rates must be adjusted to account for the actual reactivity of the system.

---

*Gay (private communication). The formation of HONO in a nonirradiated mixture of NO_2 and DEHA was unmistakable, but because these two compounds have existed in the gas phase in other chambers without rapid reaction, the results observed by Gay may be attributable to surface effects. A subsequent 5-min irradiation showed removal of both DEHA and HONO with no identifiable product buildup.

SECTION 5

CONCLUSIONS

The results of adding DEHA to chamber irradiations of HC/NO_x systems were empirically defined for propylene and n-butane.

As long as DEHA was present in the gas phase in the chamber, the physical manifestations of smog formation were retarded or inhibited. However, DEHA is an organic molecule which does react to produce "smog" itself; once it was consumed, all of the manifestations of smog production were aggravated in the test reaction systems. In particular, the chamber runs indicated that the DEHA-consumed system produced: (1) increased O_3 formation; (2) rapid conversion of NO to NO_x; (3) increased HC consumption; (4) increased PAN production; (5) aerosol in greater volume and in a size distribution that is more likely to affect visibility; and (6) a significantly different NO_x product profile. These results have significant impact on any proposed control strategy involving DEHA.

It has been suggested (4,6,16) that continual and sufficient introduction of DEHA into the urban environment could significantly lower the exposure of the urban population to smog. Under normal meterological conditions, this conclusion is probably correct. However, addition of DEHA to the urban atmosphere is much like "adding fuel to the fire." Should the concentration of DEHA drop below "adequate" levels, the adverse effects of smog on the urban population are likely to be exacerbated. In addition, these studies indicate that the impact on rural areas downwind from the urban center may be significant and undesirable. Under conditions of stagnant air over the urban center, the necessary amount of DEHA to be injected on the second and subsequent days

would have to be increased to overcome the reactivity of both the cumulative HC and NO_x emissions and the buildup of DEHA reaction products. At some point, DEHA concentrations would become unacceptable (on account of odor, etc.), or the reactivity of the total organic chemical loading would become sufficiently large to overwhelm the DEHA inhibition and produce smog effects despite the presence of DEHA.

Finally, introduction of DEHA into the atmosphere may expose the populace to some unknown NO_x product of DEHA. The runs presented above show that the NO_x profile is significantly different with DEHA added to the system. The high NO_x concentrations late in the DEHA runs cannot be accounted for by PAN, NO_2, NO, and nitric acid (HNO_3). $CH_3CH_2NO_2$ and N_2O (the major NO_x products identified by Heicklen (4)) could not be monitored because of gas chromatographic insensitivity, but studies of the response of the chemiluminescent NO_x instrument indicate that substantial concentrations of these compounds would be required to account for the observed NO_x readings. This implies that some other NO_x product (or a chemiluminescent interferent) must be formed during the reaction. An attempt to analyze these NO_x products by FTIR was unsuccessful because of experimental problems (Gay, private communication; see previous footnote). The reaction scheme in Figure 19 suggests several possible intermediate NO_x products (EtNO, DENO, $EtN(O)=CHCH_3$, etc.); Heicklen *et al.* (4) have also suggested $(C_2H_5)_2\text{-}N(O)\text{-}NO$. The possible hazards of exposure to these or other possible NO_x products of the reaction are currently unknown.

REFERENCES

1. Stephens, E. R., R. H. Linnell, and L. Reckner. Atmospheric Photochemical Reactions Inhibited by Iodine. Science 138:831, 1962.

2. Jayanty, R. K. M., R. Simonaitis, and J. Heicklen. The Inhibition of Photochemical Smog. III. Inhibition by Diethylhydroxylamine, N-Methylaniline, Triethylamine, Diethylamine, Ethylamine and Ammonia. Atmos. Environ. 8:1283, 1974.

3. Two New Approaches to Smog Control. Chemical and Engineering News 54(37): 32, 1976.

4. Stockburger, L., B. K. T. Sie, and J. Heicklen. The Inhibition of Photochemical Smog. V. Products of the Diethylhydroxylamine Inhibited Reaction. Report No. 407-75, Center for Air Environment Studies, The Pennsylvania State University, University Park, Pennsylvania, 1975.

5. Pitts, J. N., Jr., J. P. Smith, D. R. Fitz, and D. Grosjean. Enhancement of Photochemical Smog by N,N'-Diethylhydroxylamine in Polluted Ambient Air. Science 197:255, 1977.

6. Schaal, D., K. Partymiller, and J. Heicklen. The Inhibition of Photochemical Smog. VII. Inhibition of Diethylhydroxylamine at Atmospheric Concentrations. Report No. 483-77, Center for Air Environment Studies, The Pennsylvania State University, University Park, Pennsylvania, 1977.

7. Cupitt, L. T., and E. W. Corse. Status Report and DEHA Experiments. ESG-TR-78-17, Northrop Services, Inc., Research Triangle Park, North Carolina, 1978.

8. Selected Methods for the Measurement of Air Pollutants. Division of Air Pollution, Public Health Service, U.S. Department of Health, Education, and Welfare, 1965.

9. Miller, D., and C. Spicer. Measurement of Nitric Acid in Smog. J. Air Pollution Control Assoc. 25:940, 1975.

10. Schere, K., and K. Demerjian. Calculation of Selected Photolytic Rate Constants over a Diurnal Range: A Computer Algorithm. EPA-6001/4-77-015, U.S. Environmental Protection Agency, 1977.

11. Leighton, P. A. Photochemistry of Air Pollution. Academic Press, New York, 1961.

12. Finlayson, B., and J. Pitts, Jr. Photochemistry of the Polluted Troposphere. Science 192:111, 1976.

13. Reaction Rate and Photochemical Data for Atmospheric Chemistry — 1977. Circular No. 513, National Bureau of Standards, 1977.

14. Weinstock, B., and H. Niki. Carbon Monoxide Balance in Nature. Science 176:290, 1972.

15. Wang, C., L. Davis, Jr., C. Wu, S. Japur, H. Niki, and B. Weinstock. Hydroxyl Radical Concentrations Measured in Ambient Air. Science 189:797, 1975.

16. Gorse, R., Jr., R. Lii, and B. Saunders. Hydroxyl Radical Reactivity with Diethylhydroxylamine. Science 197:1365, 1977.

17. N, N-Diethylhydroxylamine: Reactions and Applications. PD-106, Product Development Department, Industrial Chemicals Division, Pennwalt Corporation, 1969.

18. Olszyna, K., and J. Heicklen. The Inhibition of Photochemical Smog. VI. The Reaction of O_3 with Diethylhydroxylamine. Report No. 405-75, Center for Air Environment Studies, The Pennsylvania State University, University Park, Pennsylvania, 1975.

APPENDIX

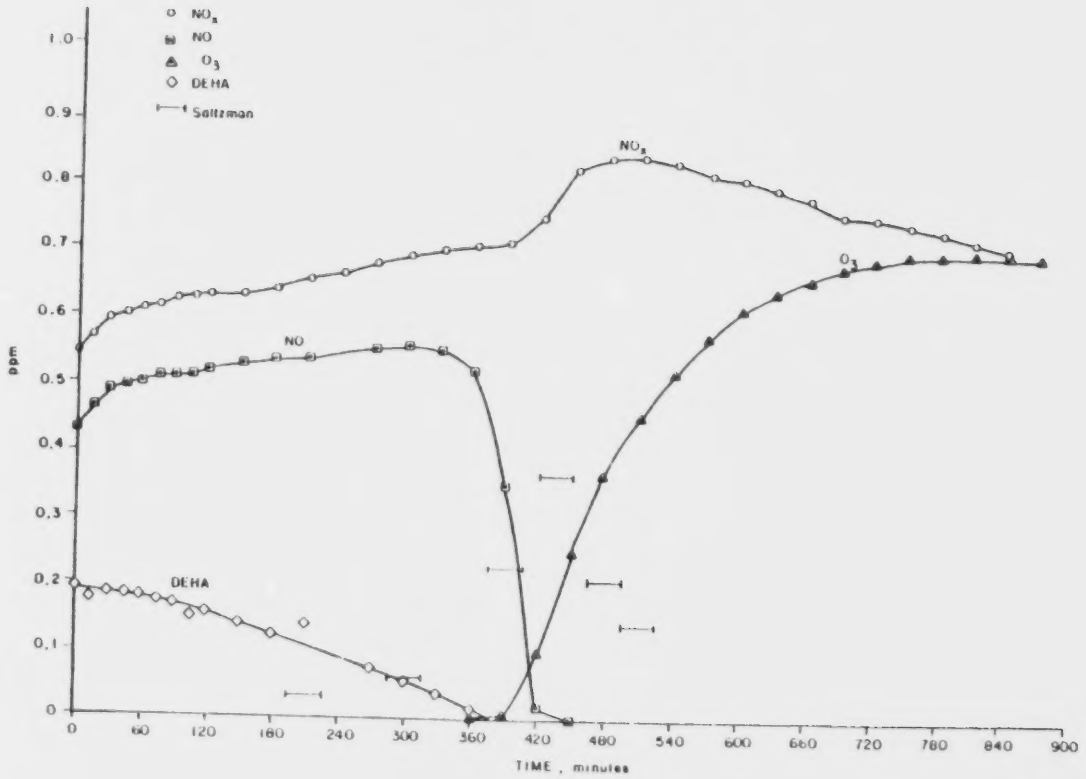

Figure A-1. Reaction profiles of DEHA-NO_x system.

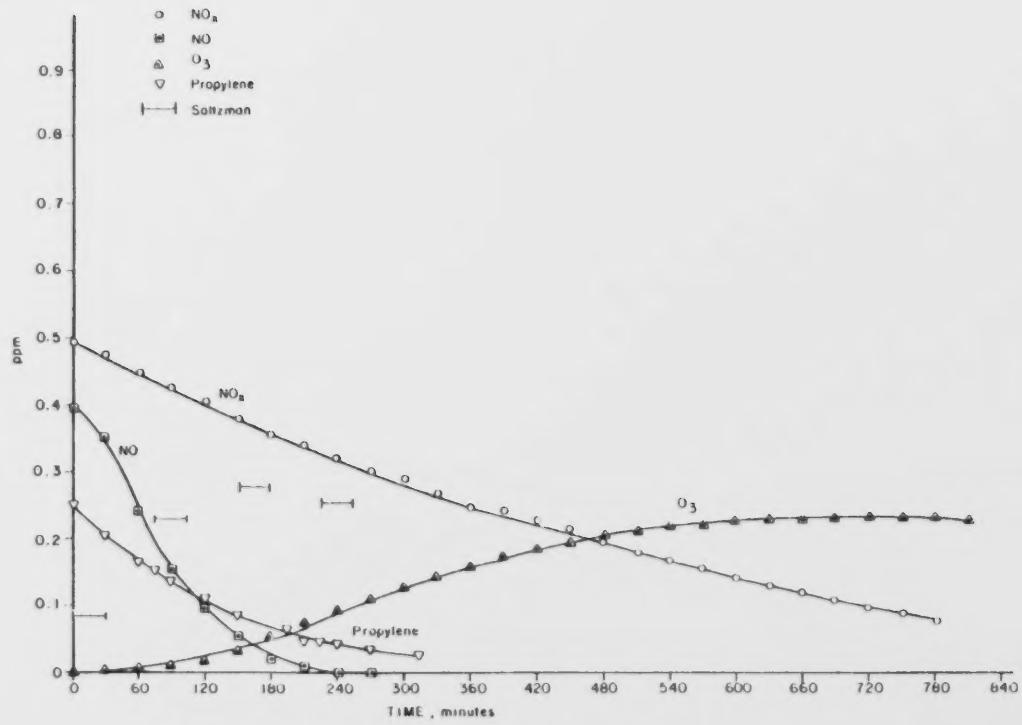

Figure A-2. Reaction profiles of 0.25 ppm propylene-NO_x system.

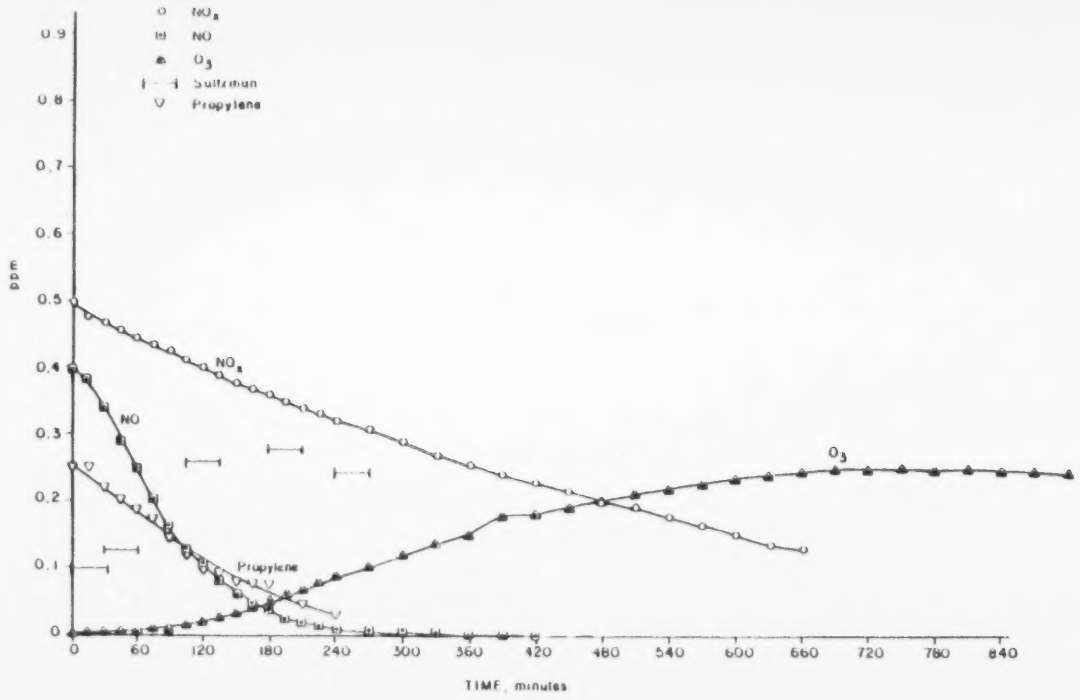

Figure A-3. Reaction profiles of 0.25 ppm propylene-NO_x system.

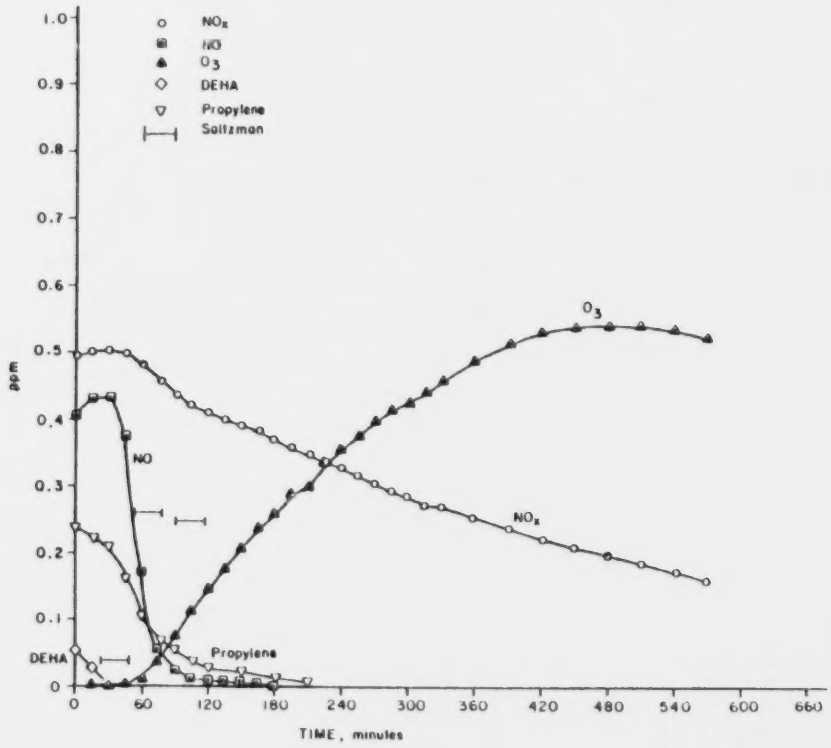

Figure A-4. Reaction profiles of 0.24 ppm propylene-NO_x-DEHA system.

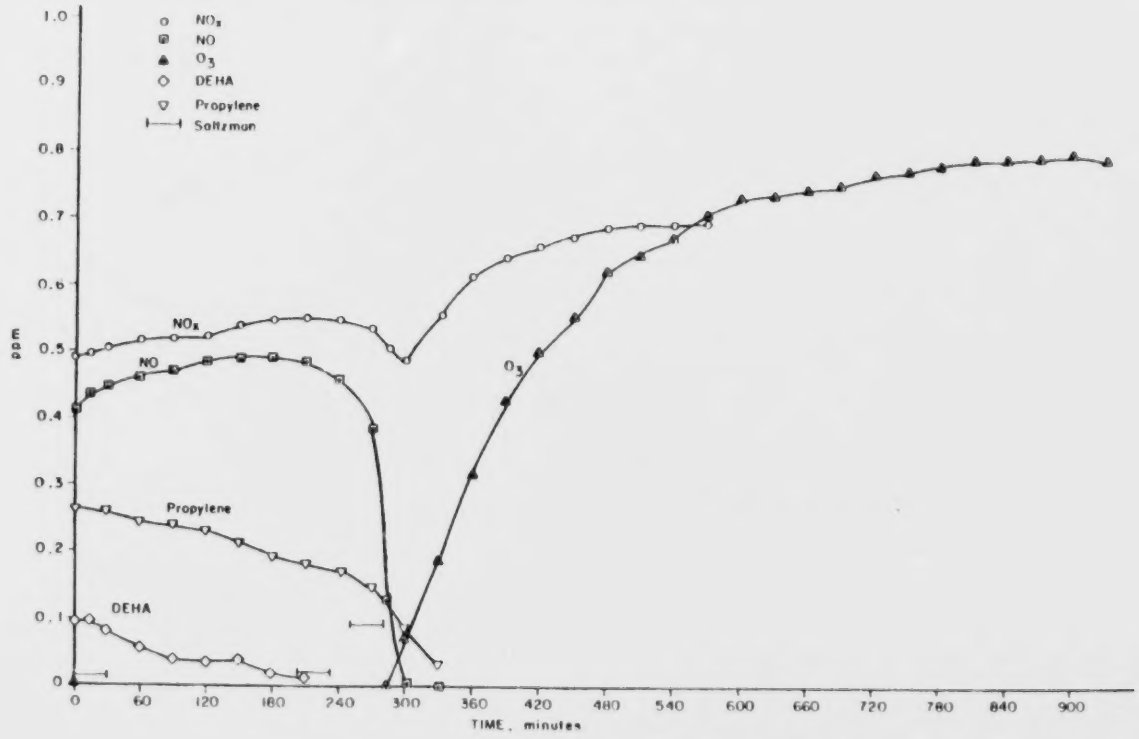

Figure A-5. Reaction profiles of 0.26 ppm propylene-NO_x-DEHA system.

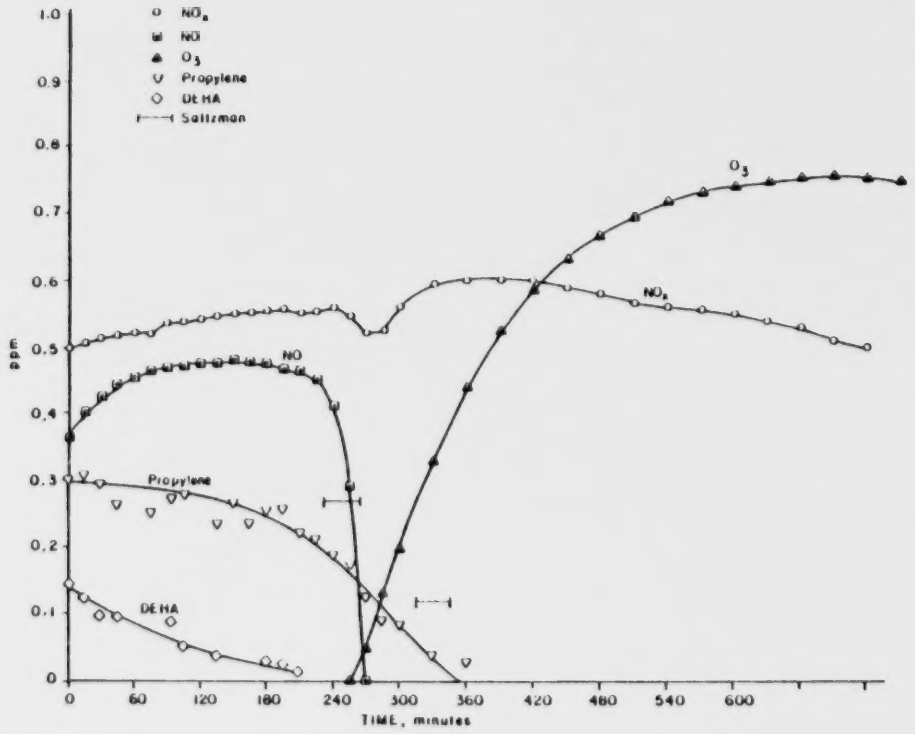

Figure A-6. Reaction profiles of 0.30 ppm propylene-NO_x-DEHA system.

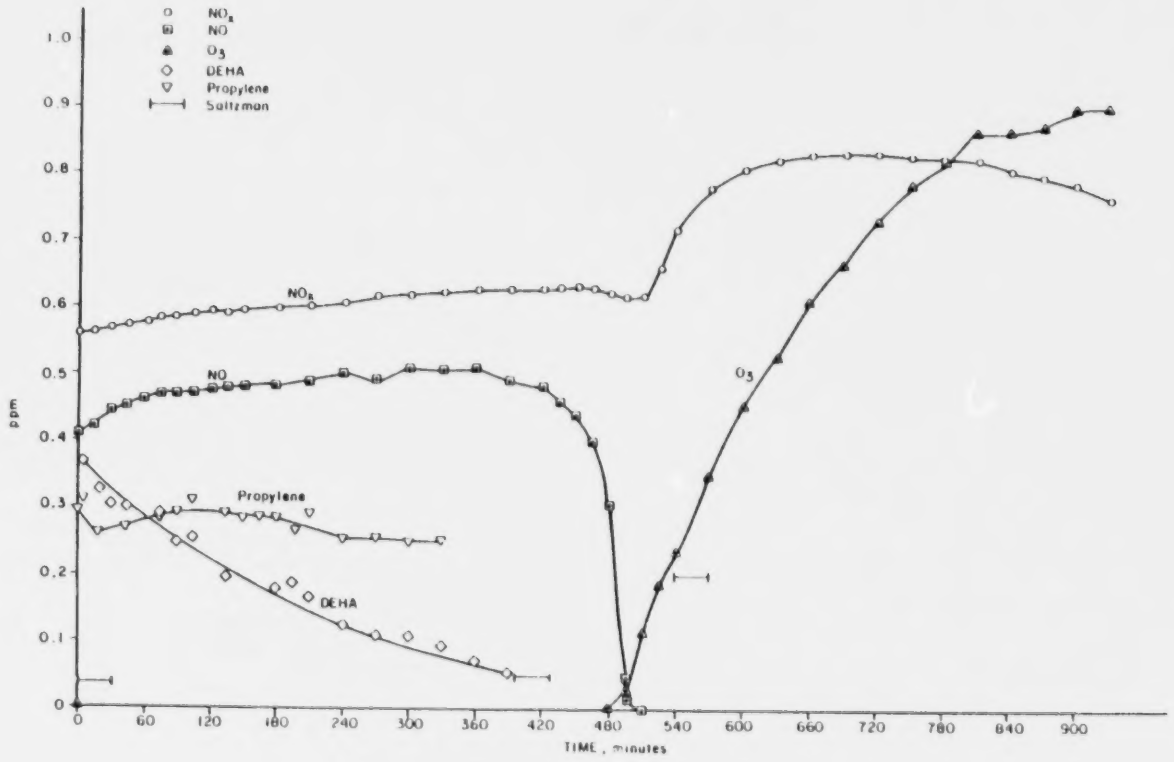

Figure A-7. Reaction profiles of 0.30 ppm propylene-NO_x-DEHA system.

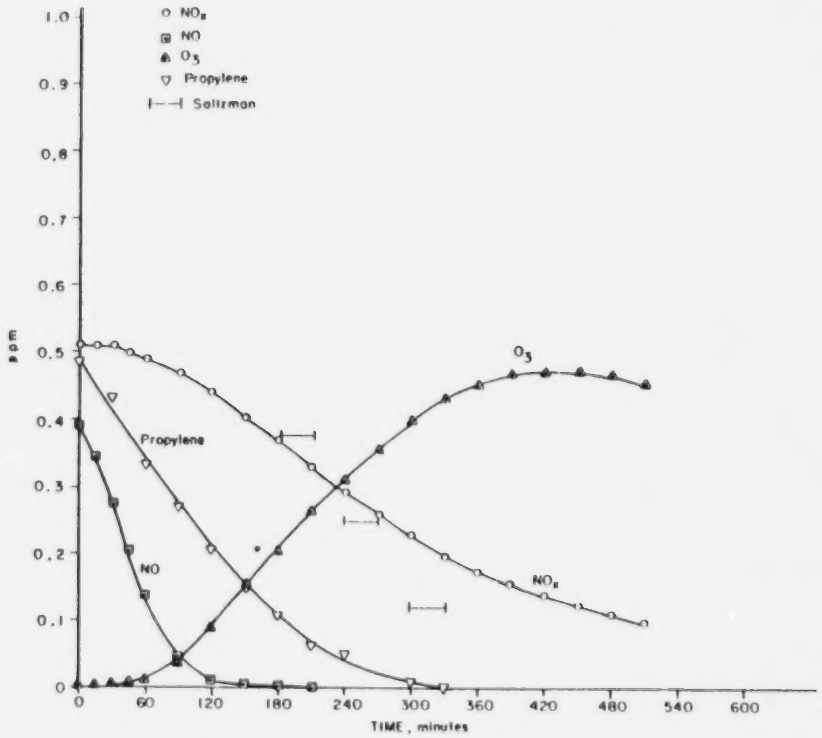

Figure A-8. Reaction profiles of 0.49 ppm propylene-NO_x system.

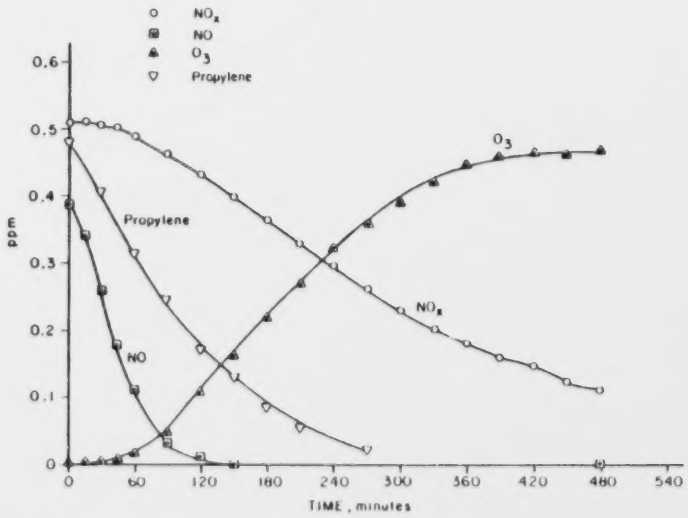

Figure A-9. Reaction profiles of 0.48 ppm propylene-NO_x system.

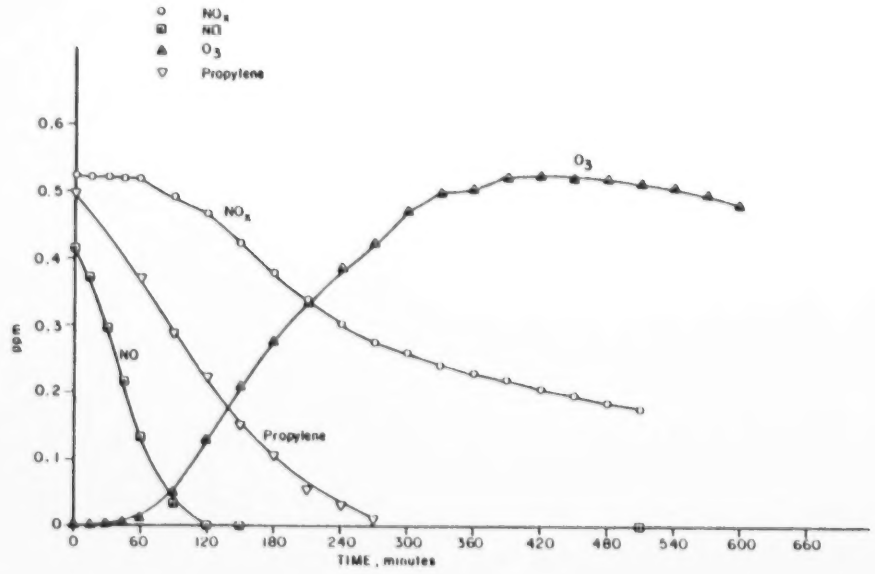

Figure A-10. Reaction profiles of 0.50 ppm propylene-NO_x system.

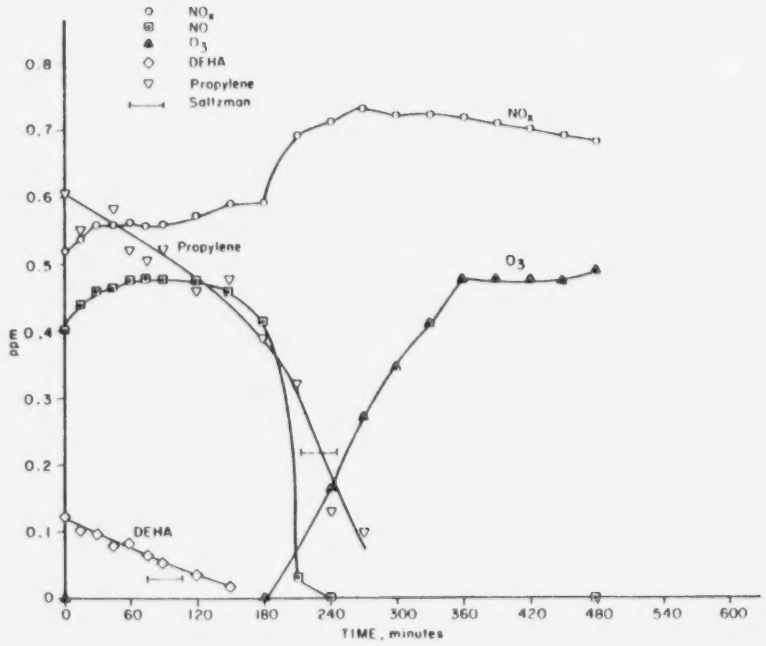

Figure A-11. Reaction profiles of 0.60 ppm propylene-NO_x-DEHA system.

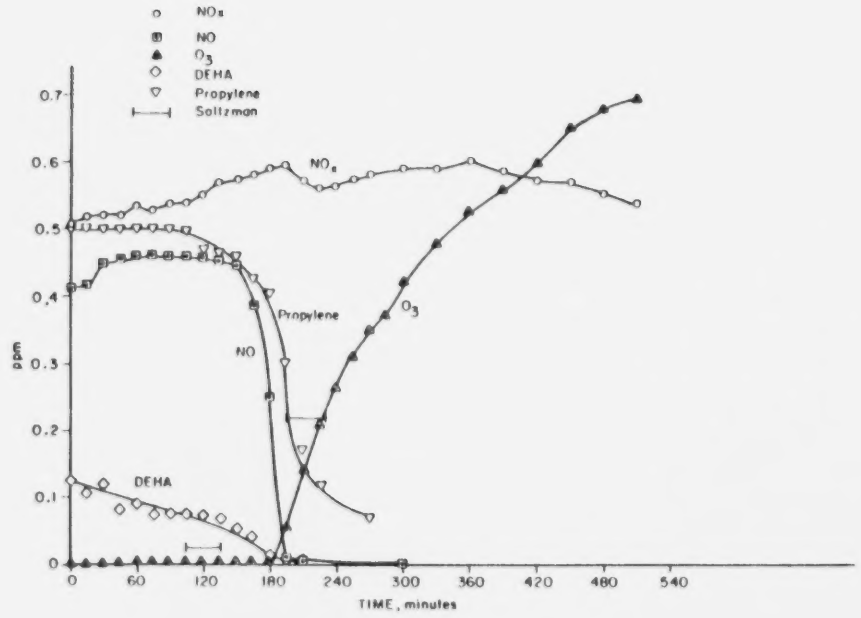

Figure A-12. Reaction profiles of 0.50 ppm propylene-NO_x-DEHA system.

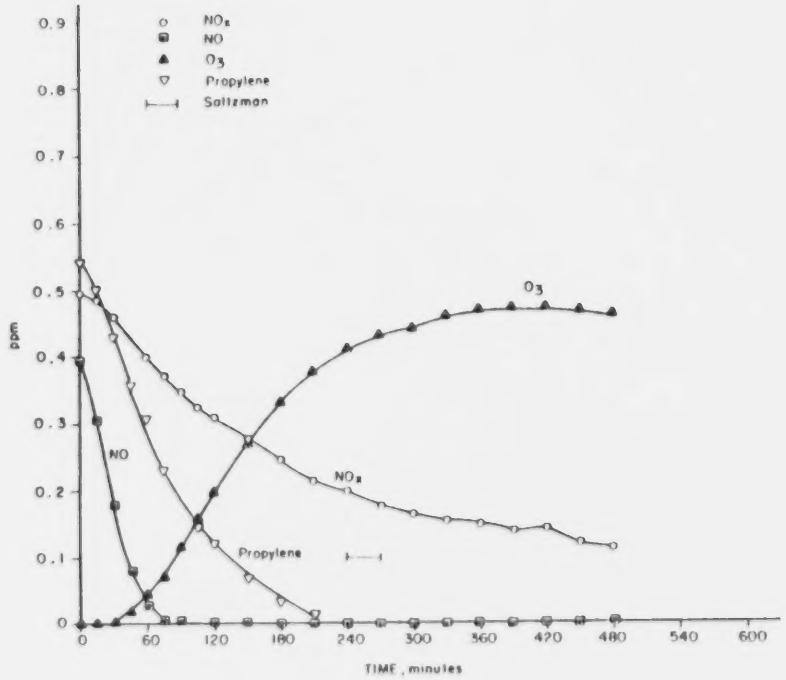

Figure A-13. Reaction profiles of 0.54 ppm propylene-NO_x system.

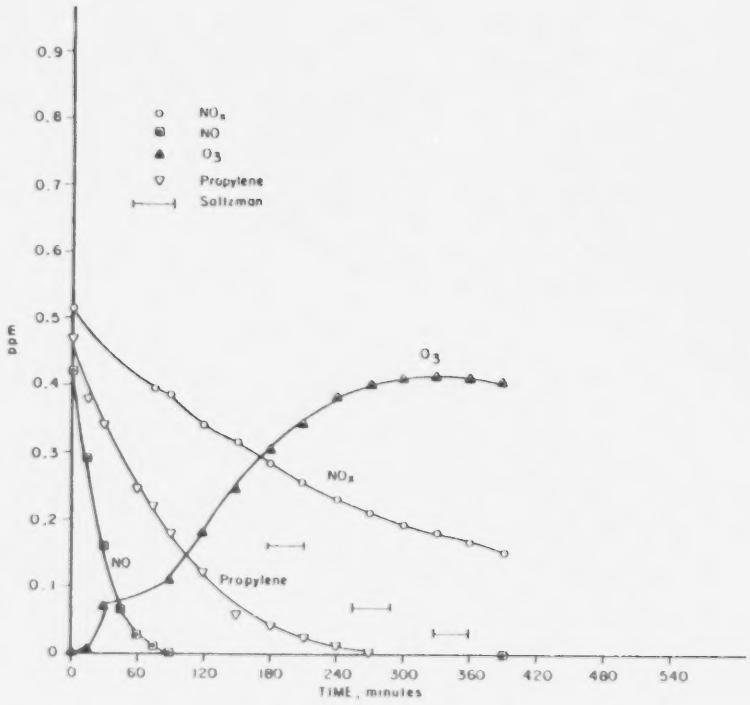

Figure A-14. Reaction profiles of 0.47 ppm propylene-NO_x system.

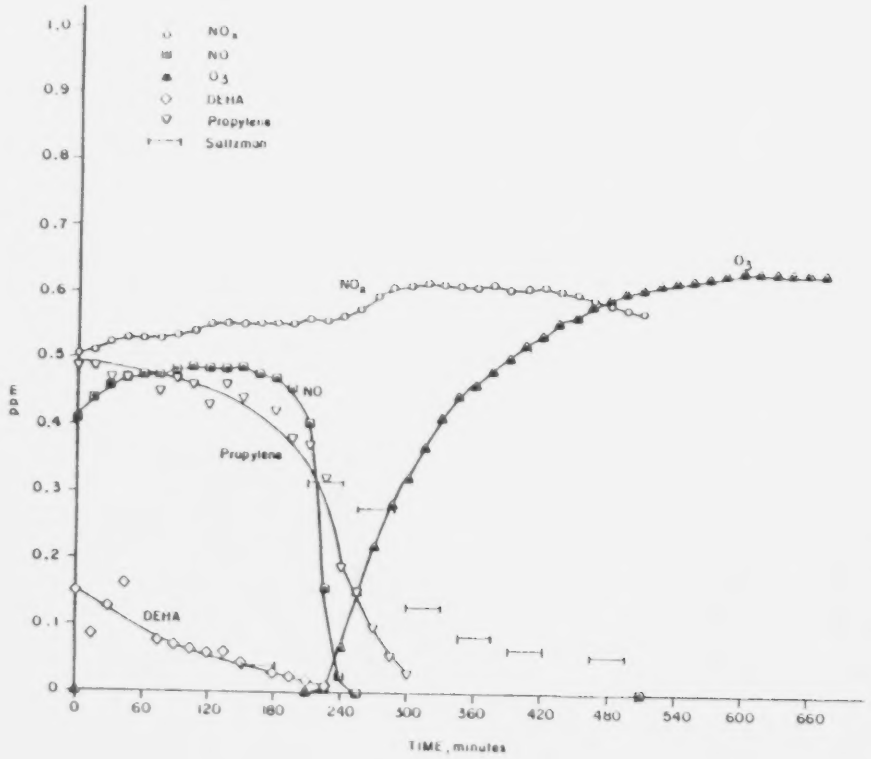

Figure A-15. Reaction profiles of 0.50 ppm propylene-NO_x-DEHA system.

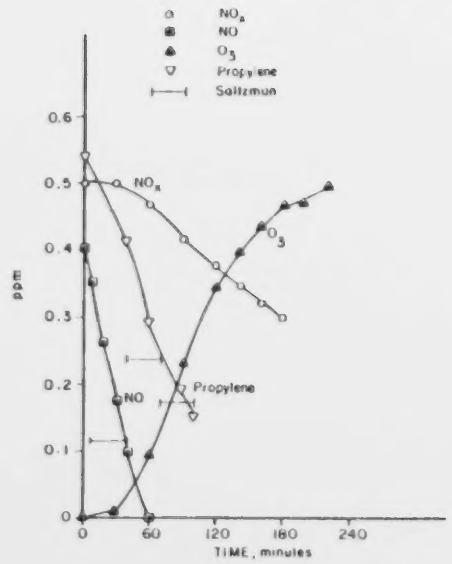

Figure A-16. Reaction profiles of 0.54 ppm propylene-NO_x system.

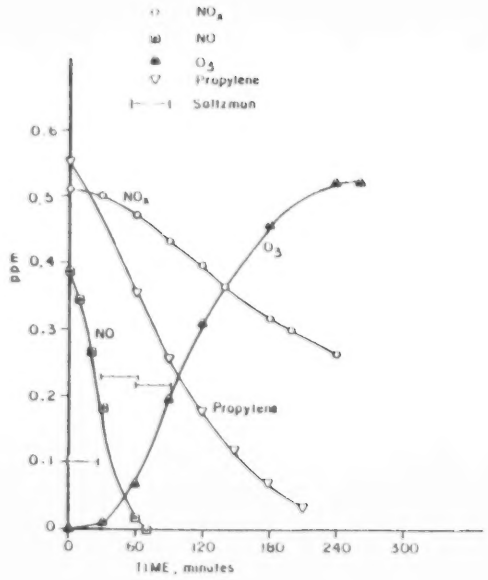

Figure A-17. Reaction profiles of 0.55 ppm propylene-NO_x system.

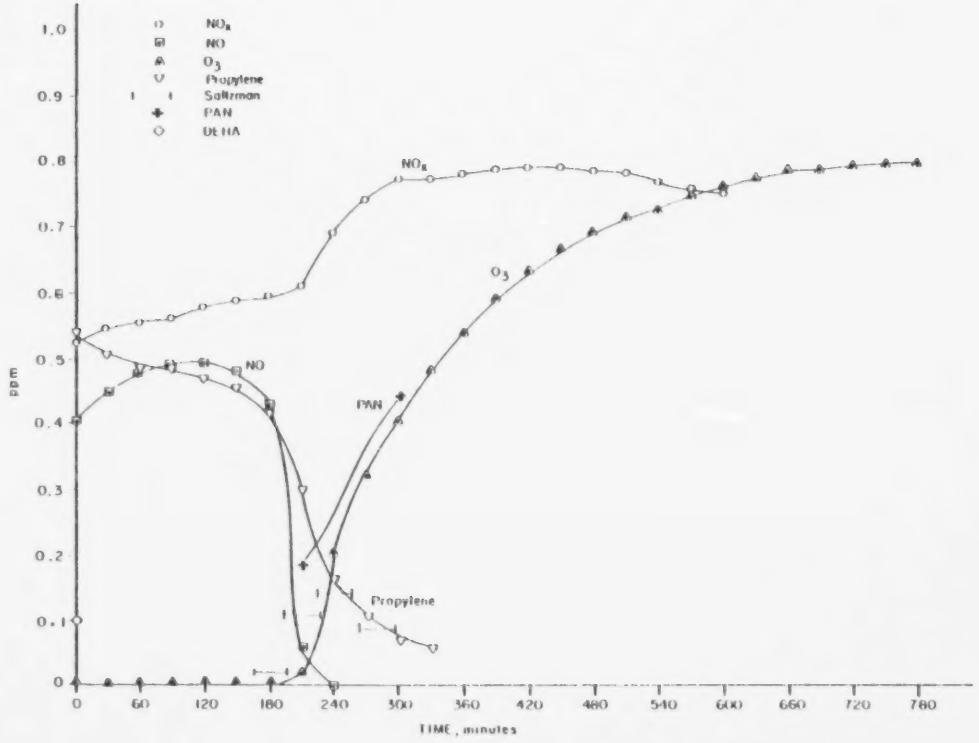

Figure A-18. Reaction profiles of 0.54 ppm propylene-NO_x-DEHA system.

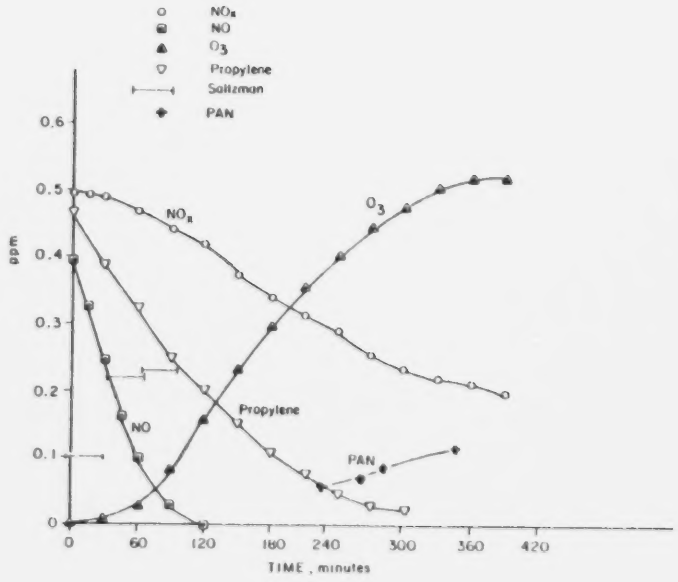

Figure A-19. Reaction profiles of 0.47 ppm propylene-NO_x system.

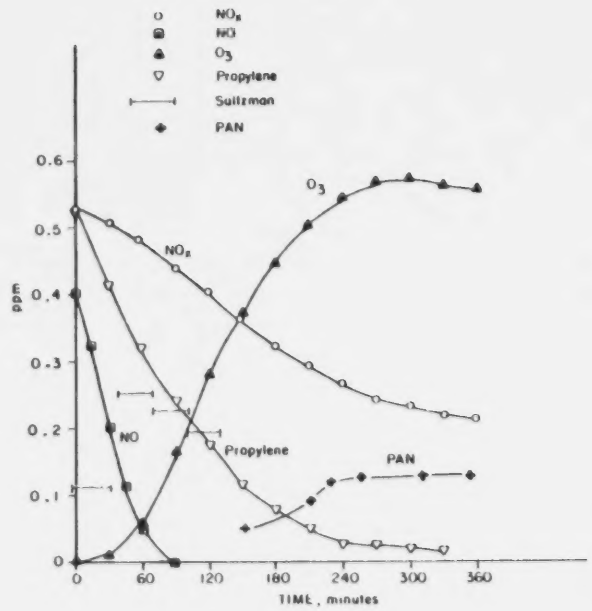

Figure A-20. Reaction profiles of 0.52 ppm propylene-NO_x system.

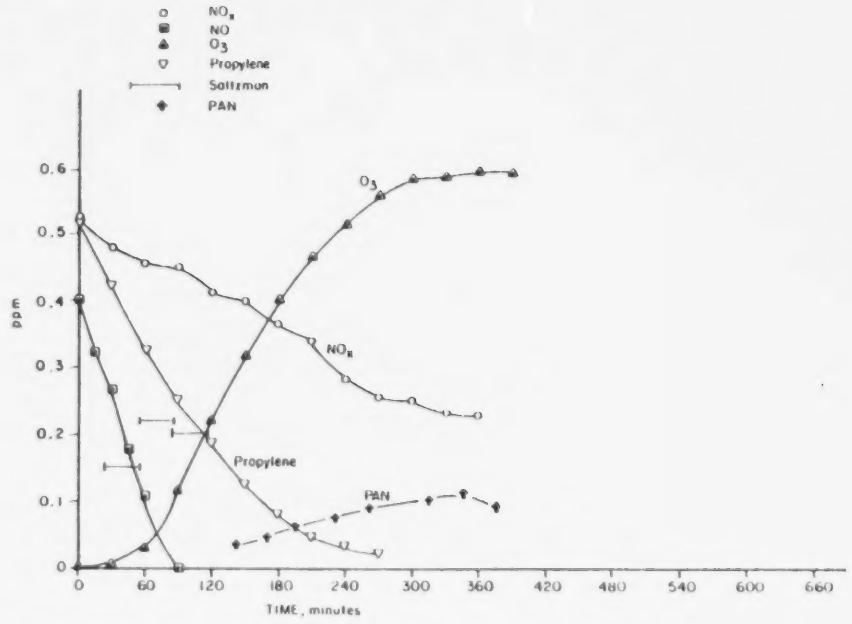

Figure A-21. Reaction profiles of 0.52 ppm propylene-NO_x system.

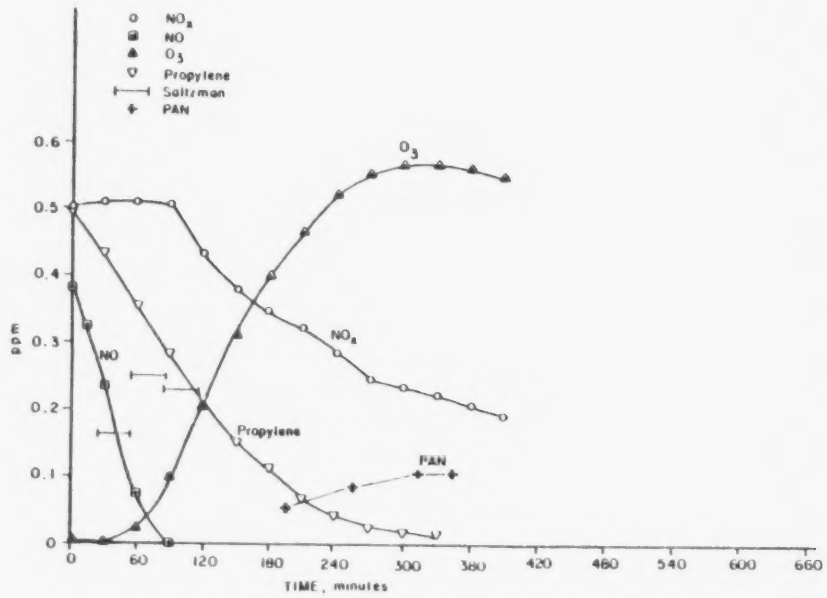

Figure A-22. Reaction profiles of 0.50 ppm propylene-NO_x system.

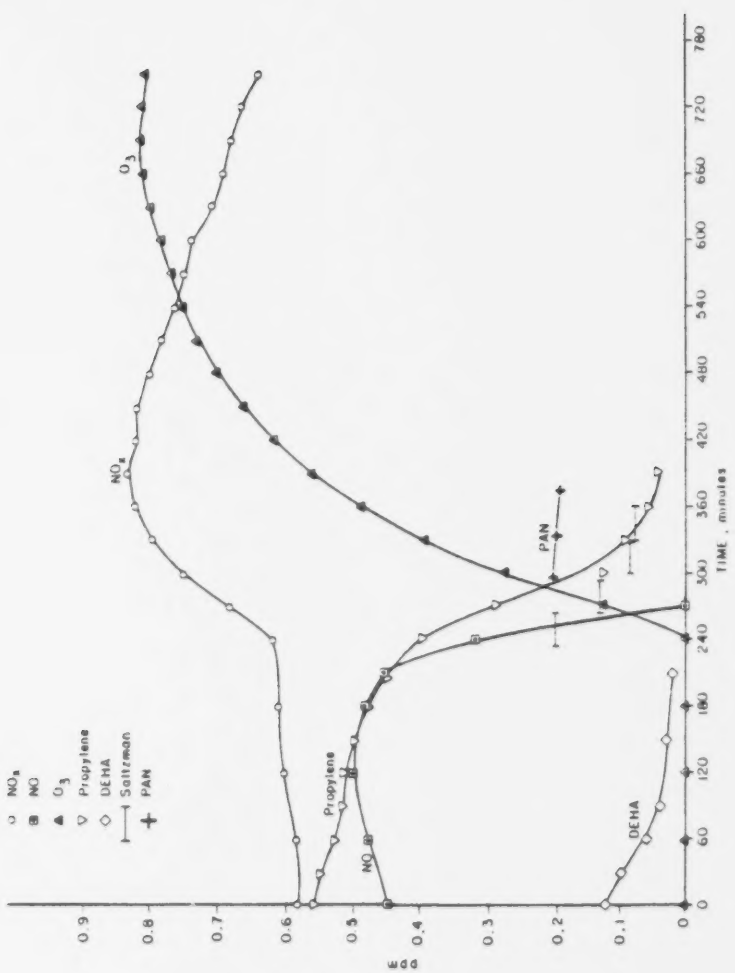

Figure A-23. Reaction profiles of 0.55 ppm propylene-NO_x-DEHA system.

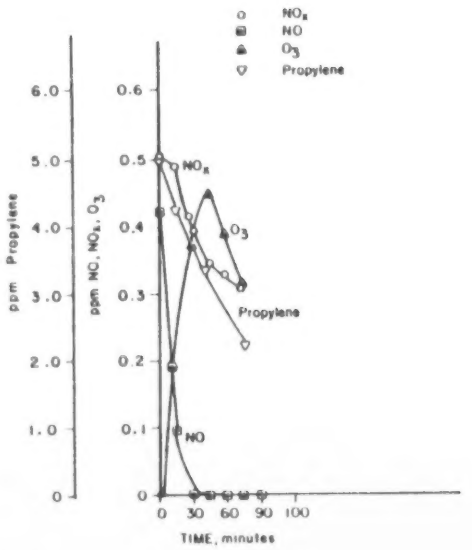

Figure A-24. Reaction profiles of 5.0 ppm propylene-NO_x system.

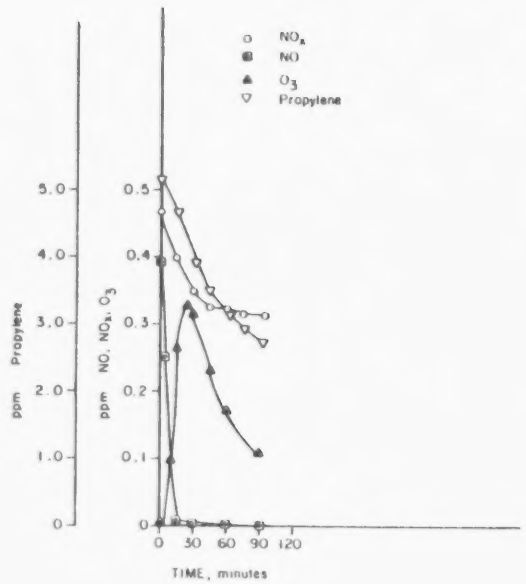

Figure A-25. Reaction profiles of 5.2 ppm propylene-NO_x system.

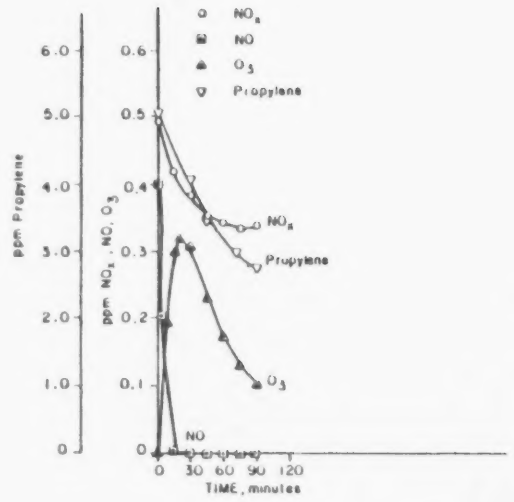

Figure A-26. Reaction profiles of 5.1 ppm propylene-NO_x system.

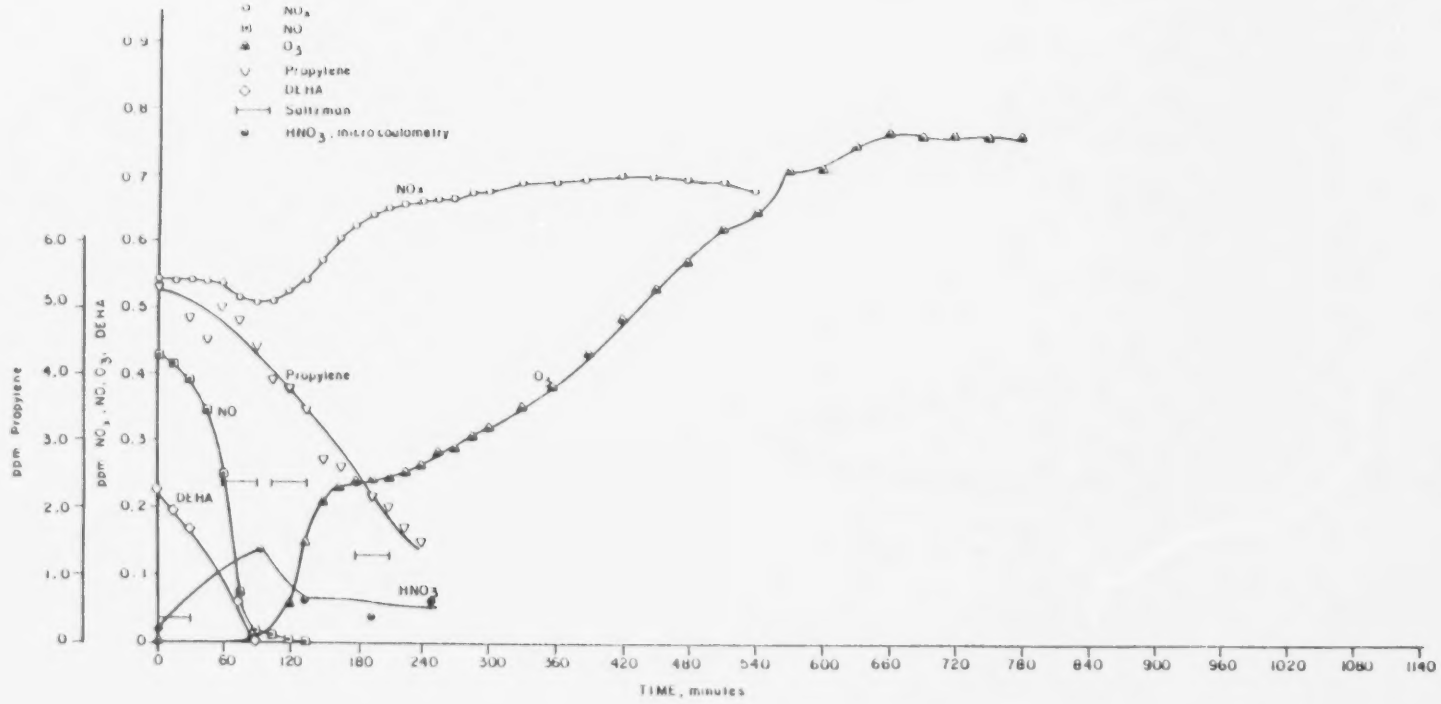

Figure A-27. Reaction profiles of 5.3 ppm propylene-NO_x-DEHA system.

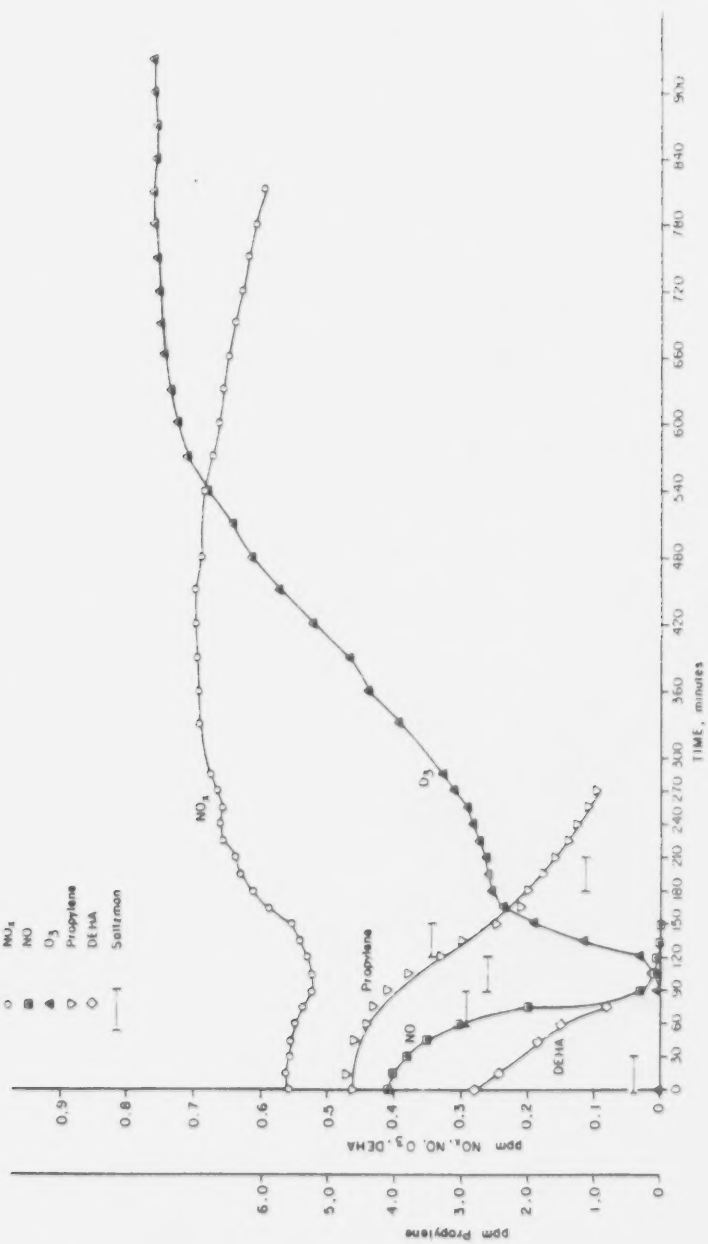

Figure A-28. Reaction profiles of 4.7 ppm propylene-NO_x-DEHA system.

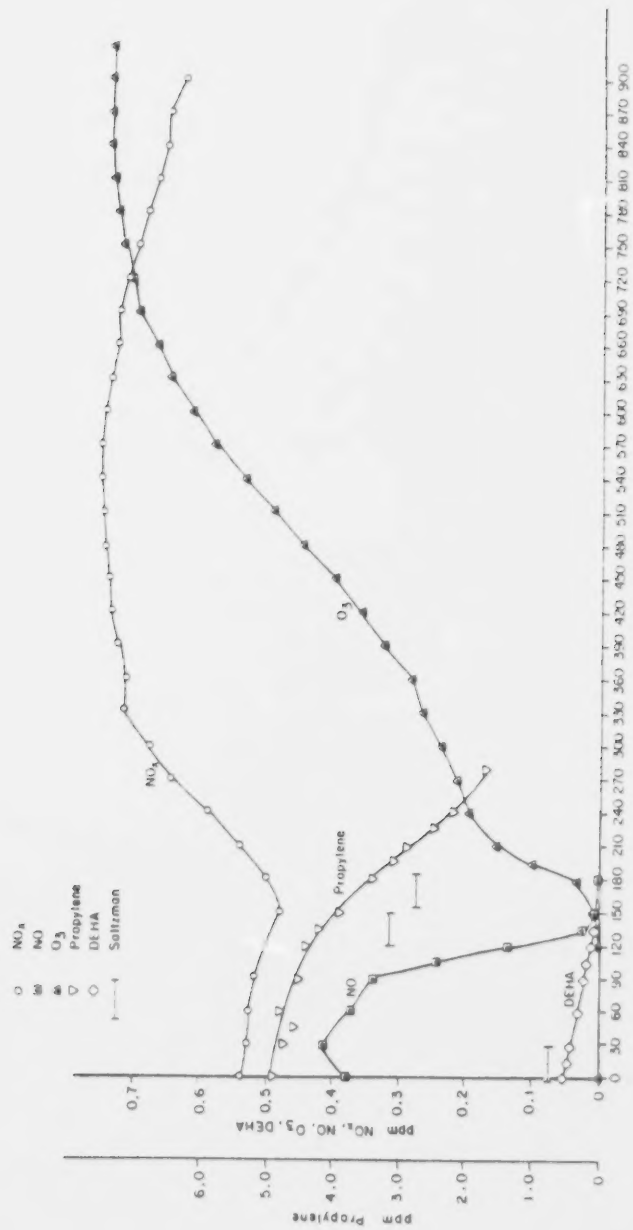

Figure A-29. Reaction profiles of 4.9 ppm propylene-NO_x-DEHA system.

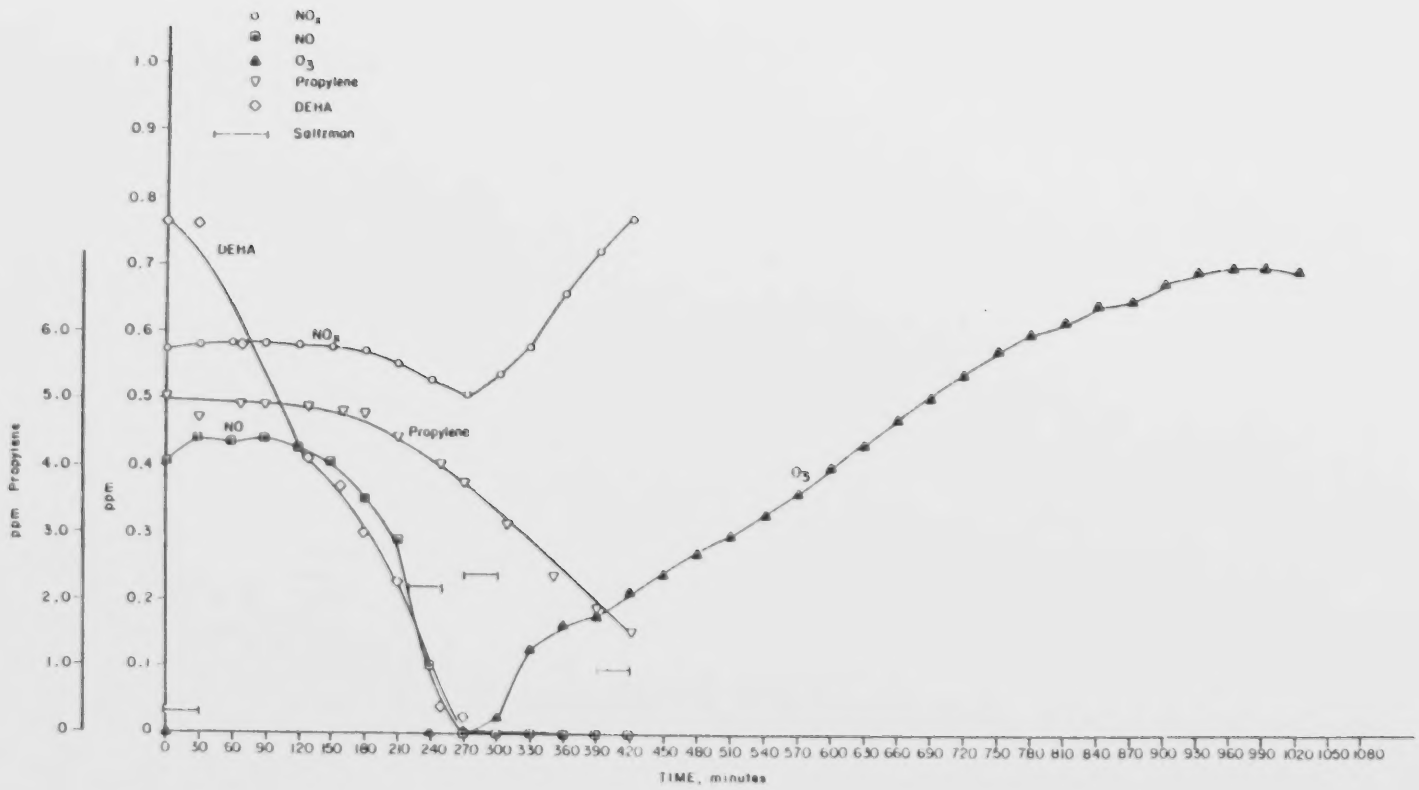

Figure A-30. Reaction profiles of 5.0 ppm propylene-NO_x-DEHA system.

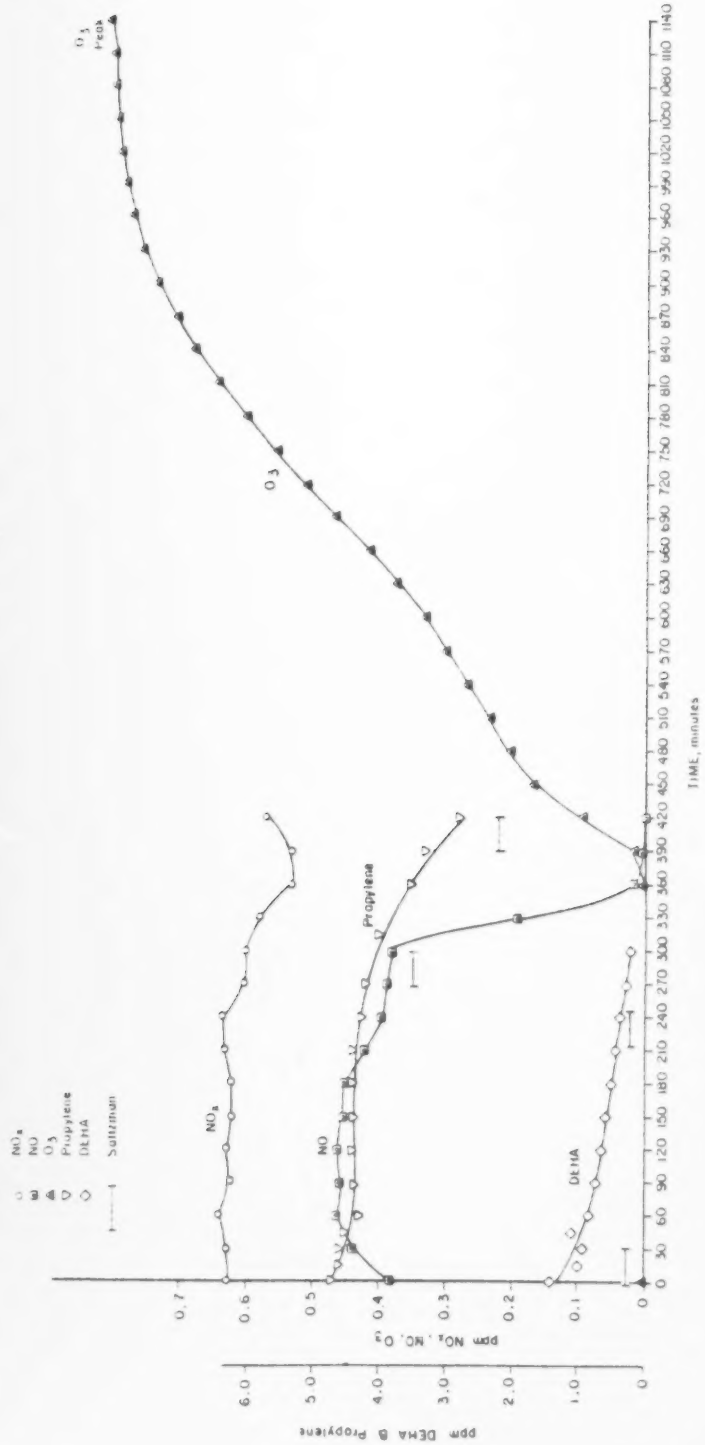

Figure A-31. Reaction profiles of 4.7 ppm propylene-NO_x-DEHA system.

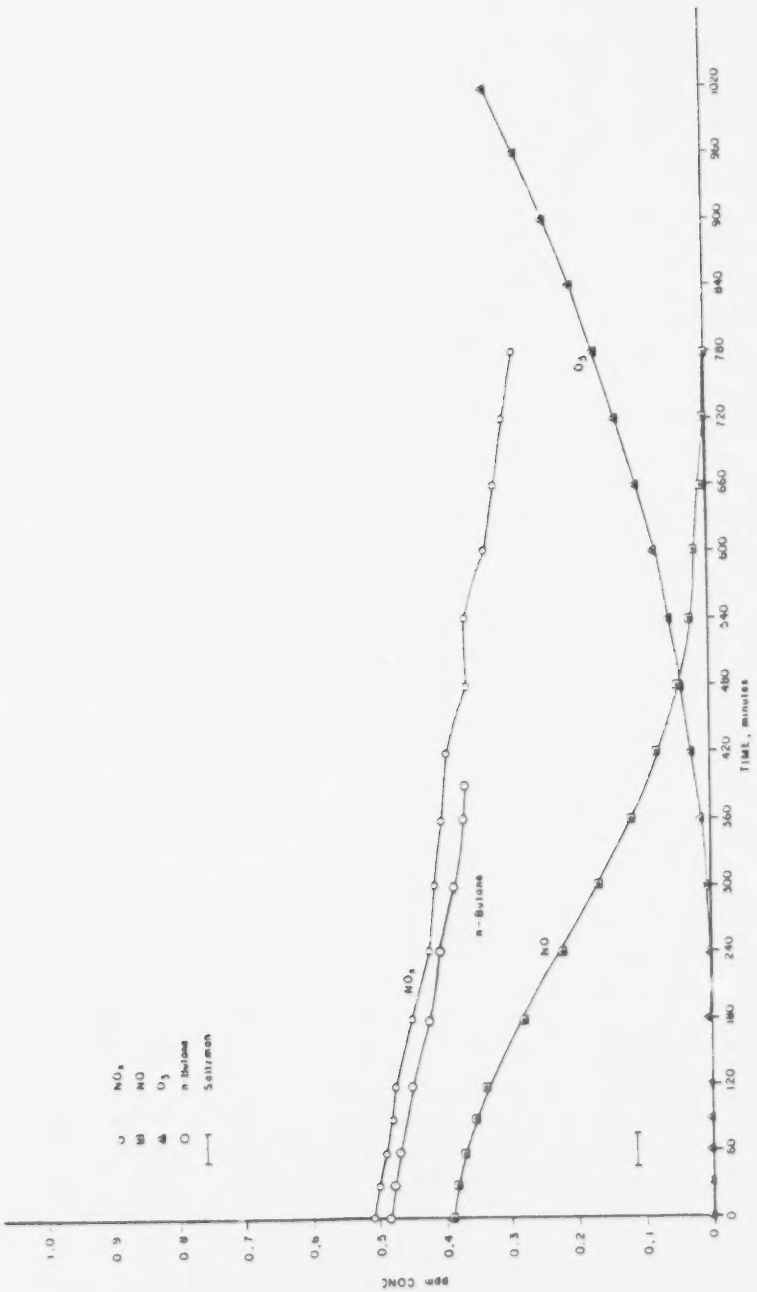

Figure A-32. Reaction profiles of 0.49 ppm n-butane-NO_x system.

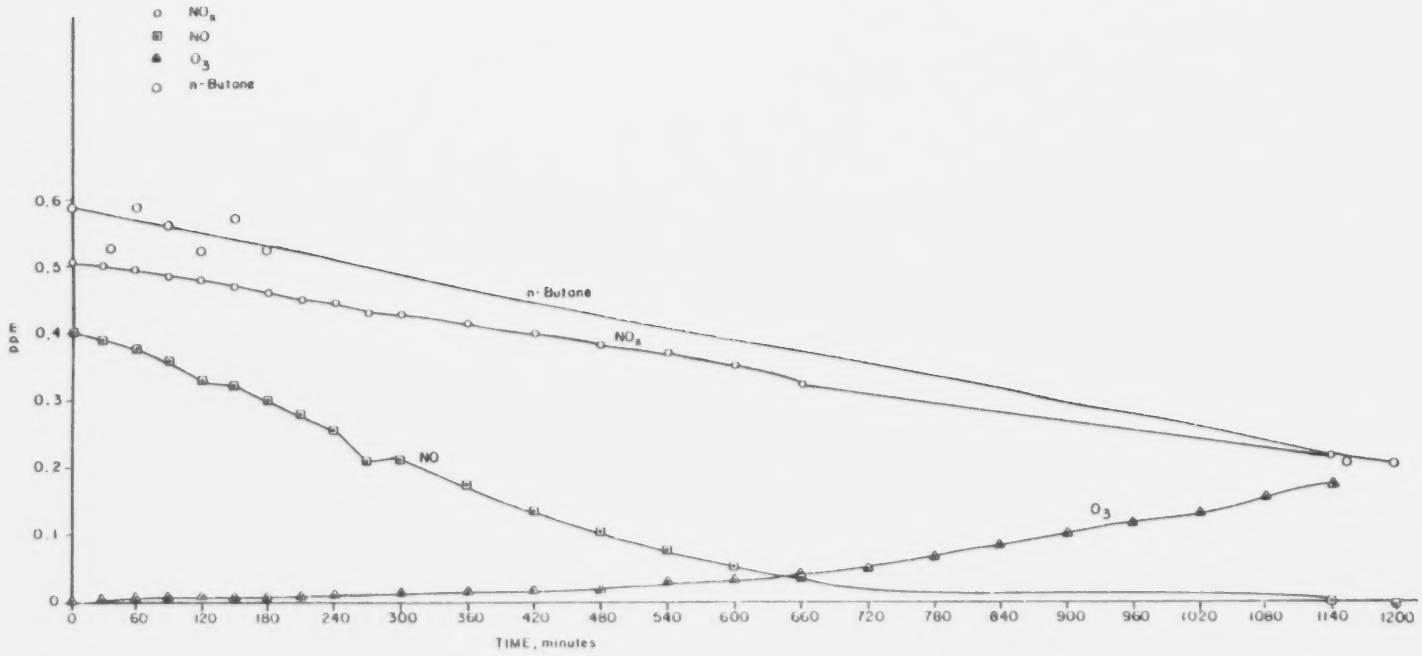

Figure A-33. Reaction profiles of 0.59 n-butane-NO_x system.

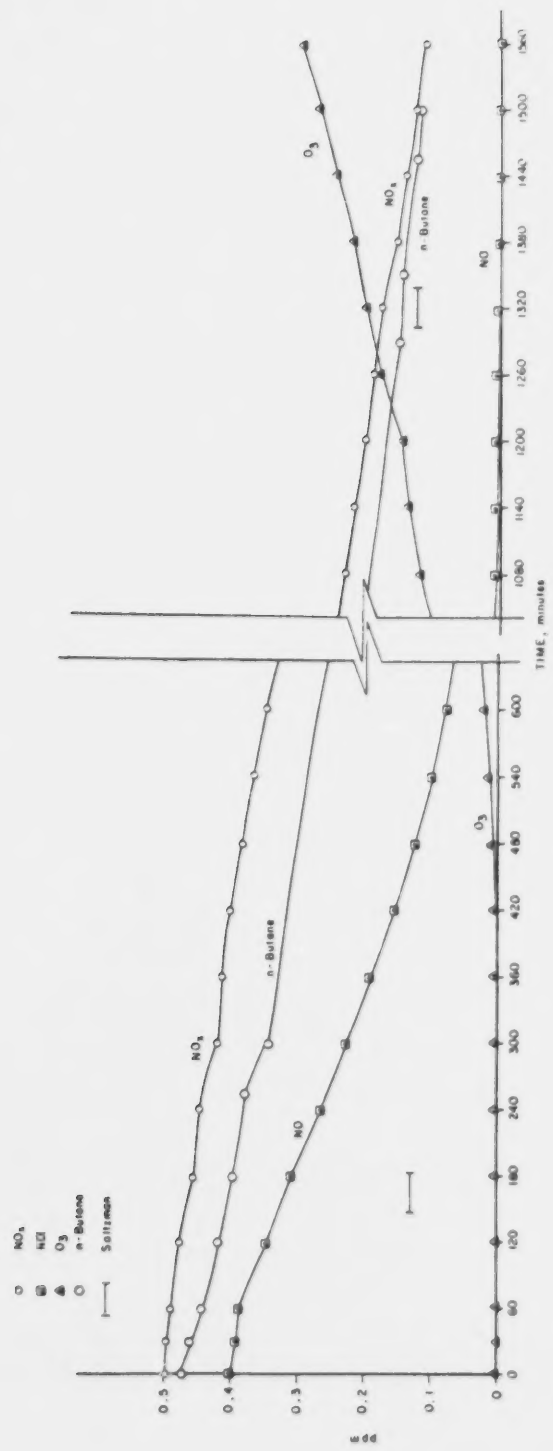

Figure A-34. Reaction profiles of 0.48 ppm n-butane-NO_x system.

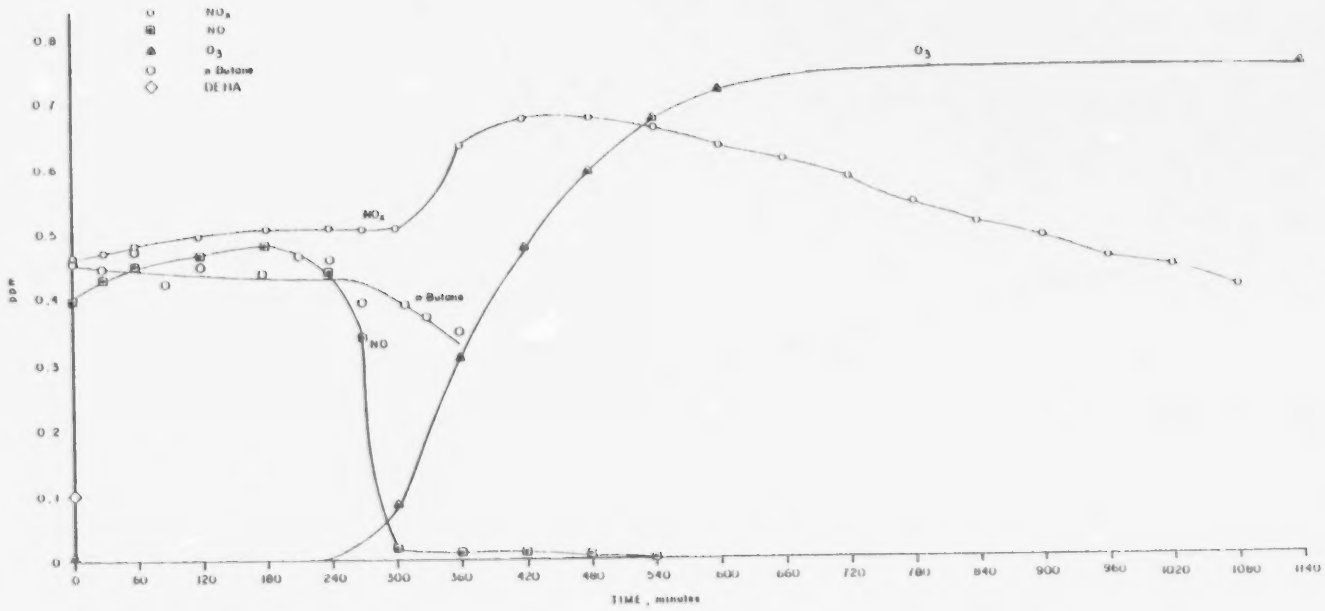

Figure A-35. Reaction profiles of 0.46 ppm n-butane-NO_x-DEHA system.

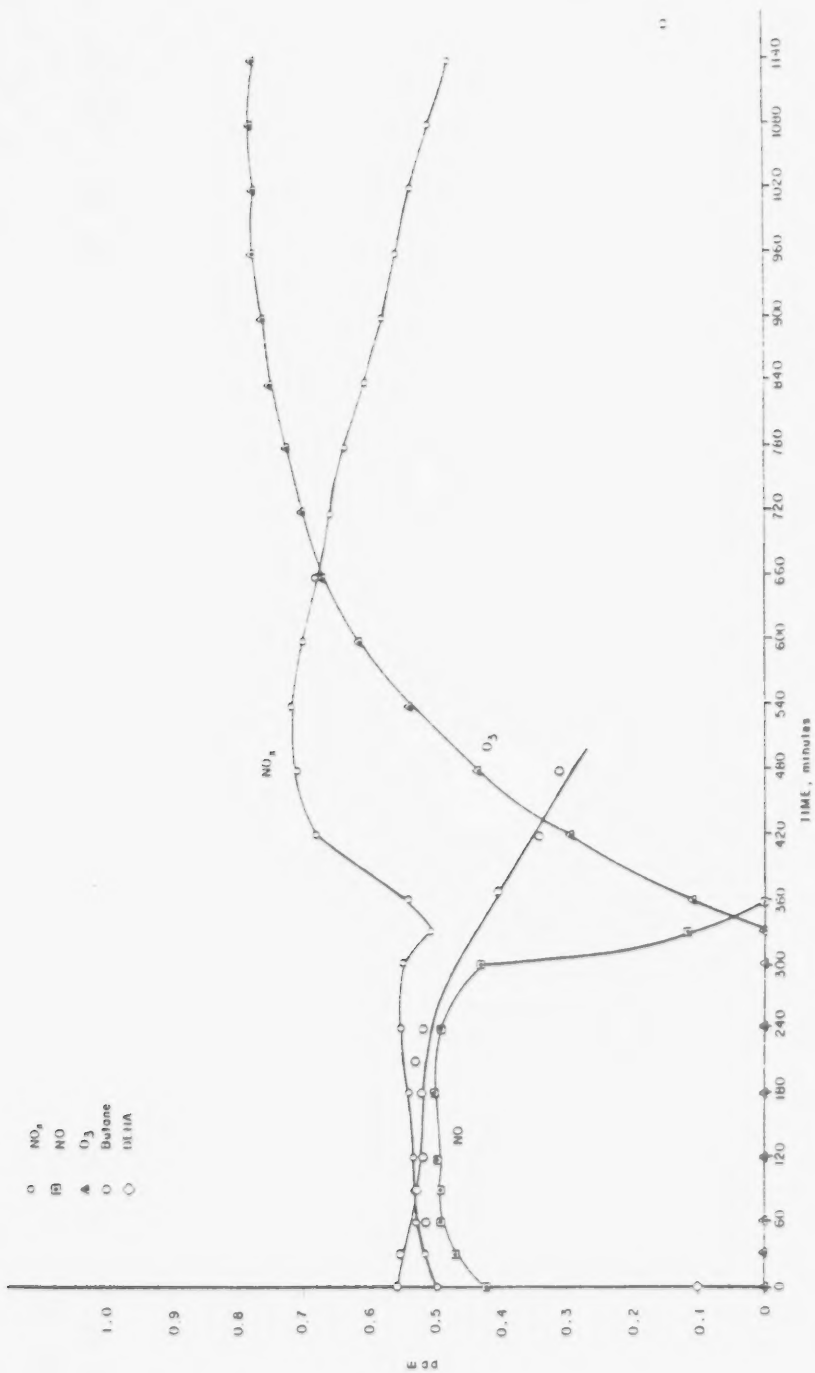

Figure A-36. Reaction profiles of 0.55 ppm n-butane-NO_x-DEHA system.

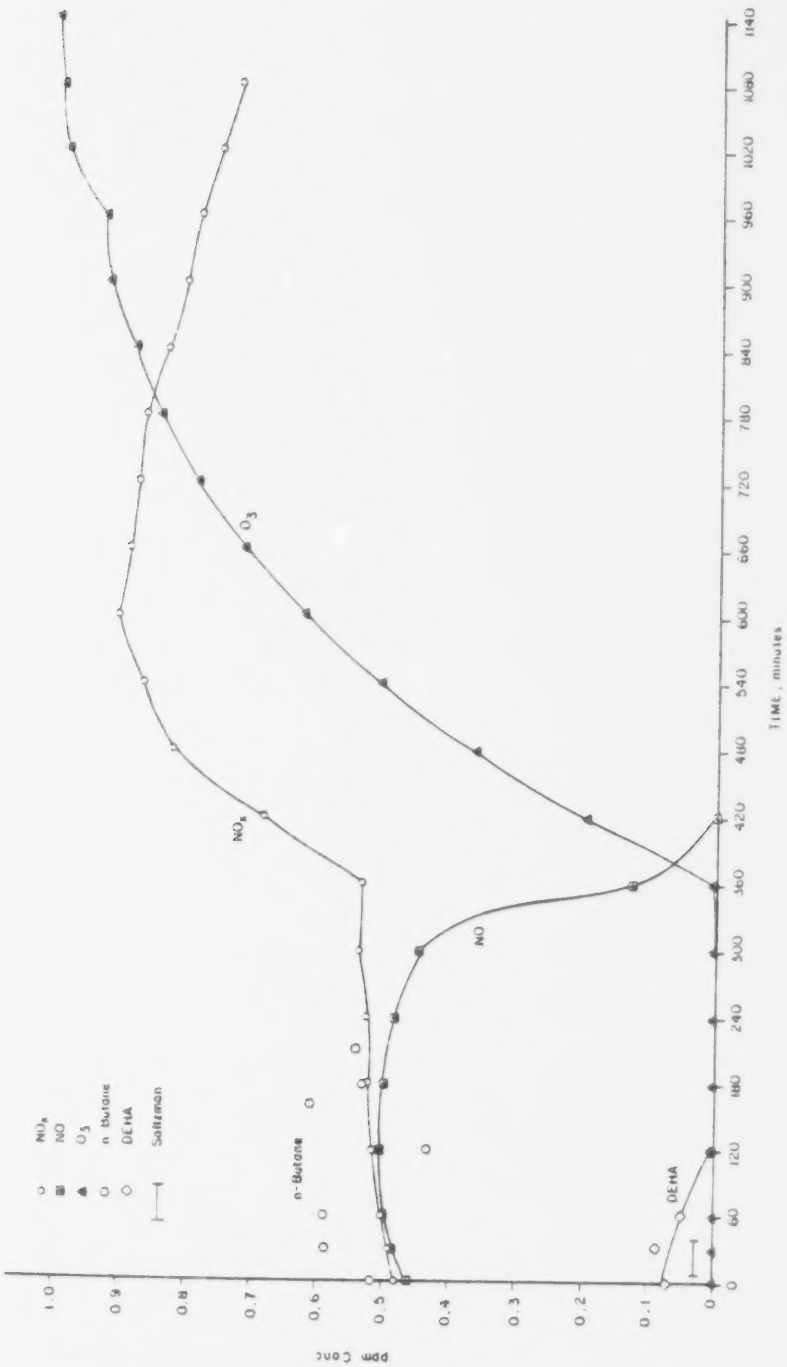

Figure A-37. Reaction profiles of 0.59 ppm n-butane-NO_x-DEHA system.

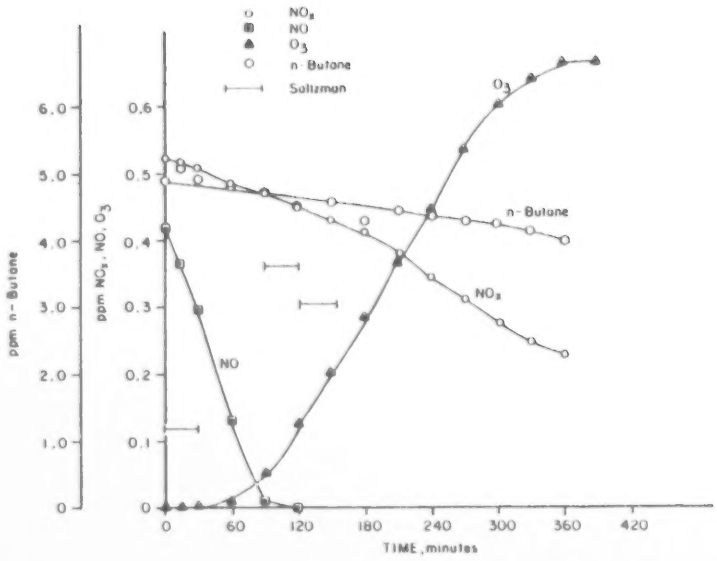

Figure A-38. Reaction profiles of 4.9 ppm n-butane-NO_x system.

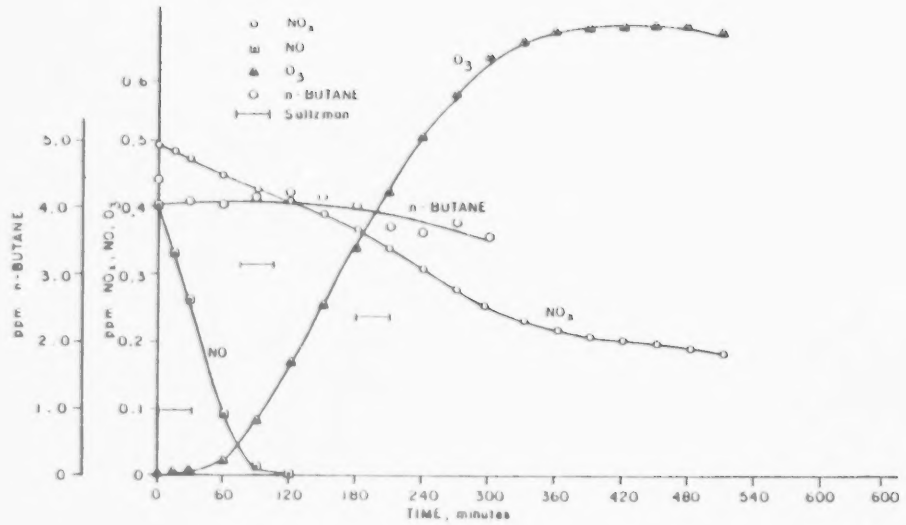

Figure A-39. Reaction profiles of 4.9 ppm n-butane-NO_x system.

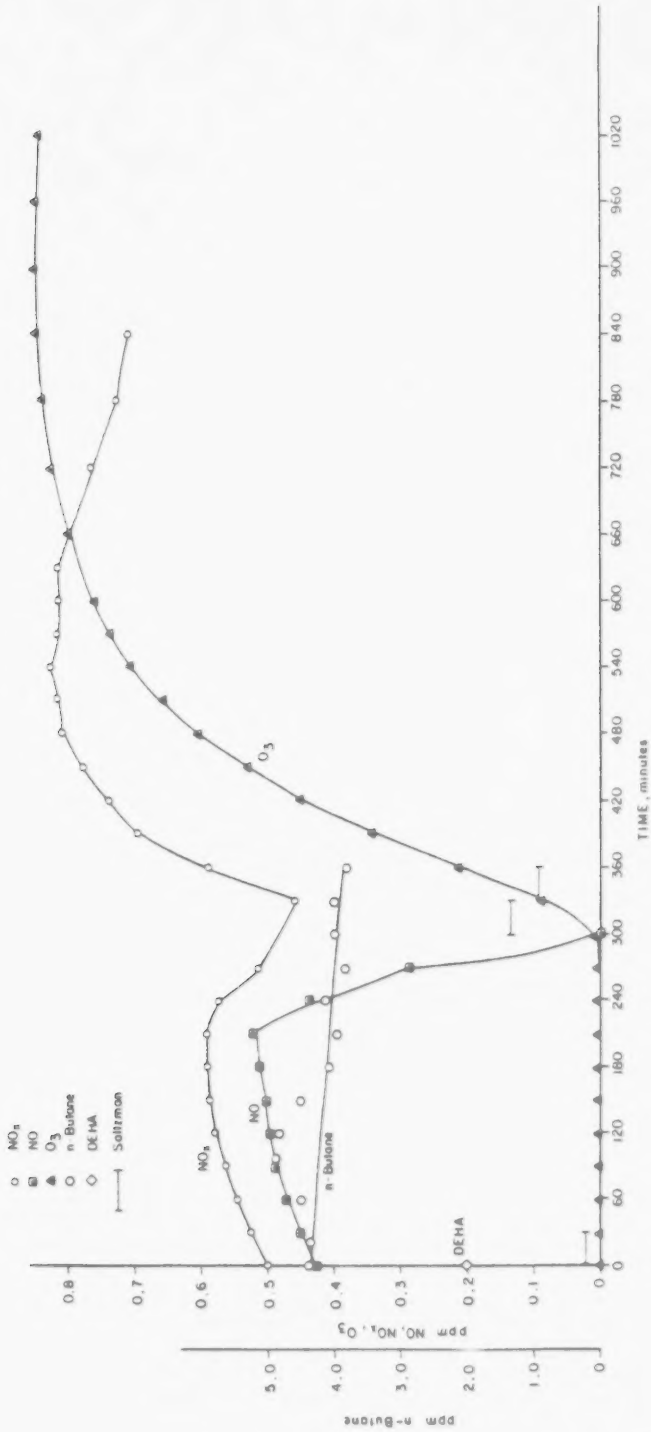

Figure A-40. Reaction profiles of 4.3 ppm n-butane-NO_x-DEHA system.

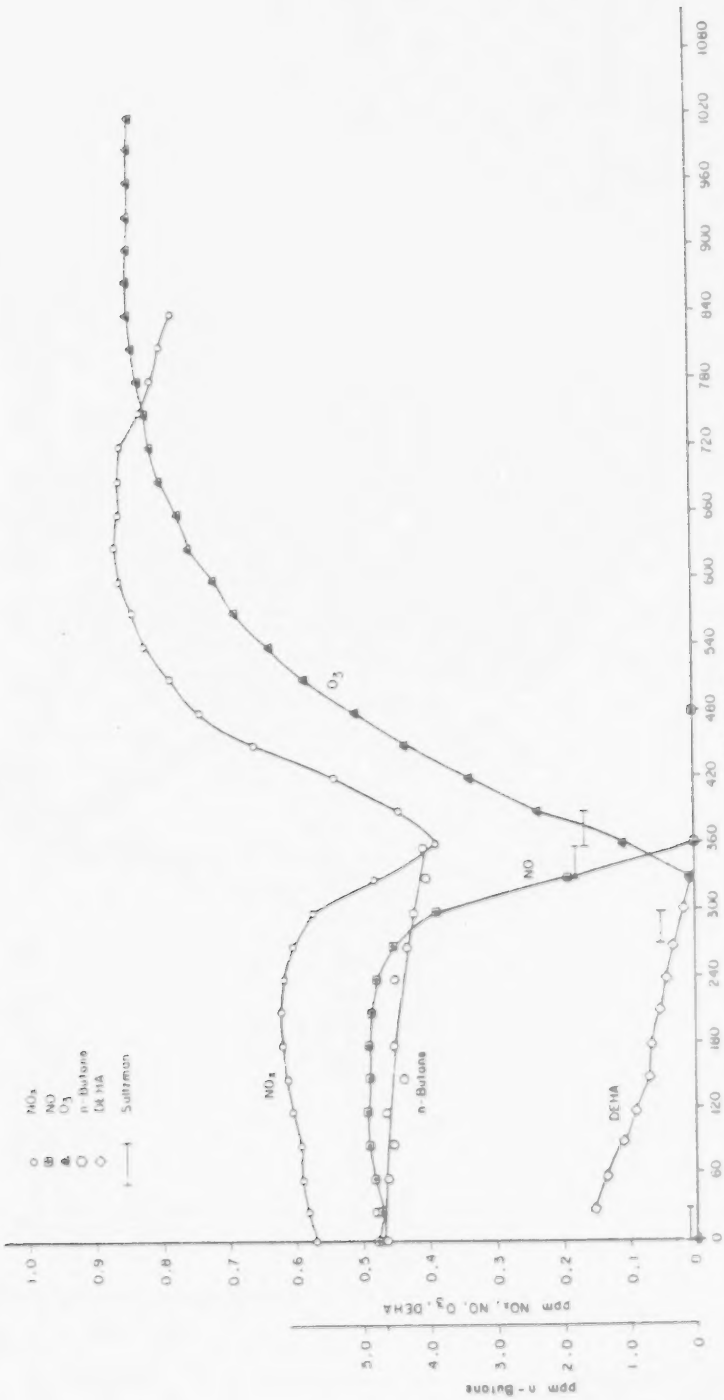

Figure A-41. Reaction profiles of 4.7 ppm n-butane-NO_x-DEHA system.

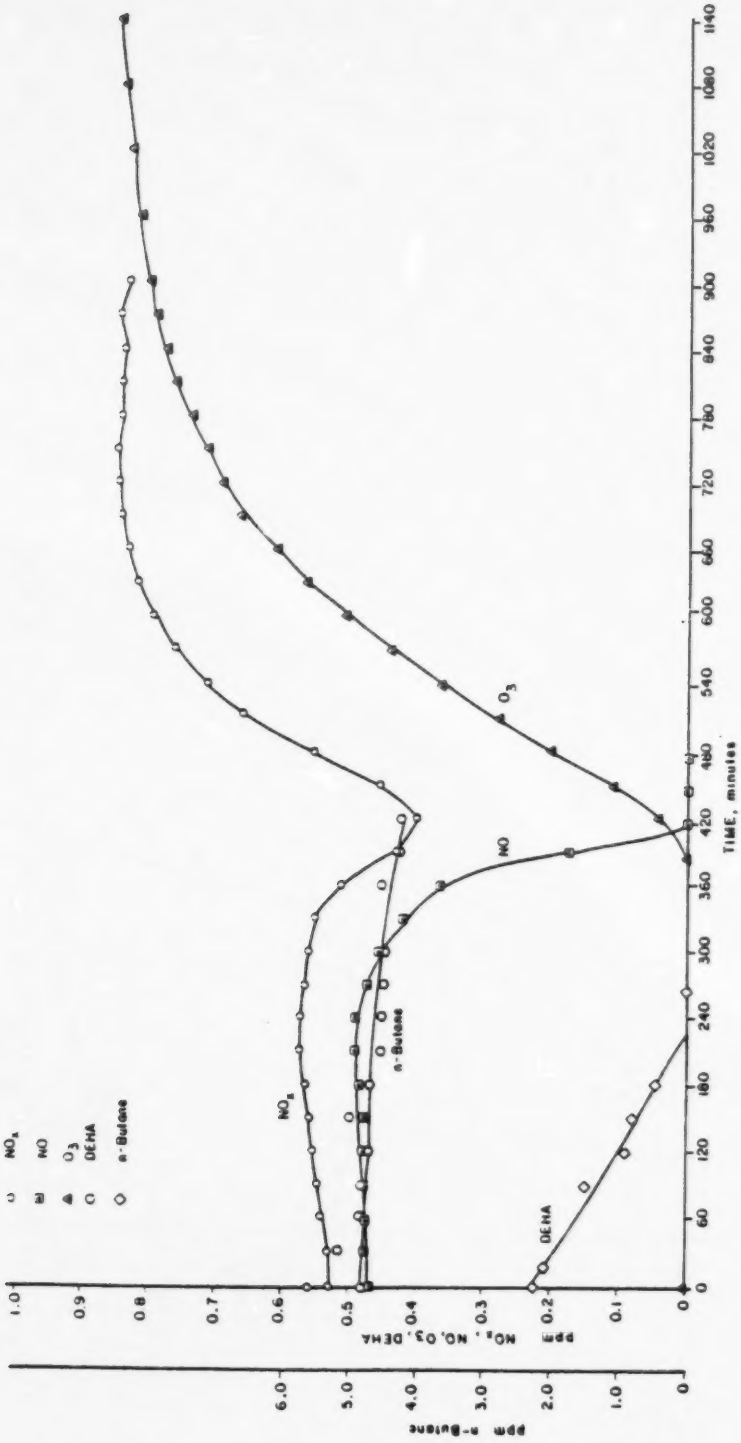

Figure A-42. Reaction profiles of 4.8 ppm n-butane-NO_x-DEHA system.

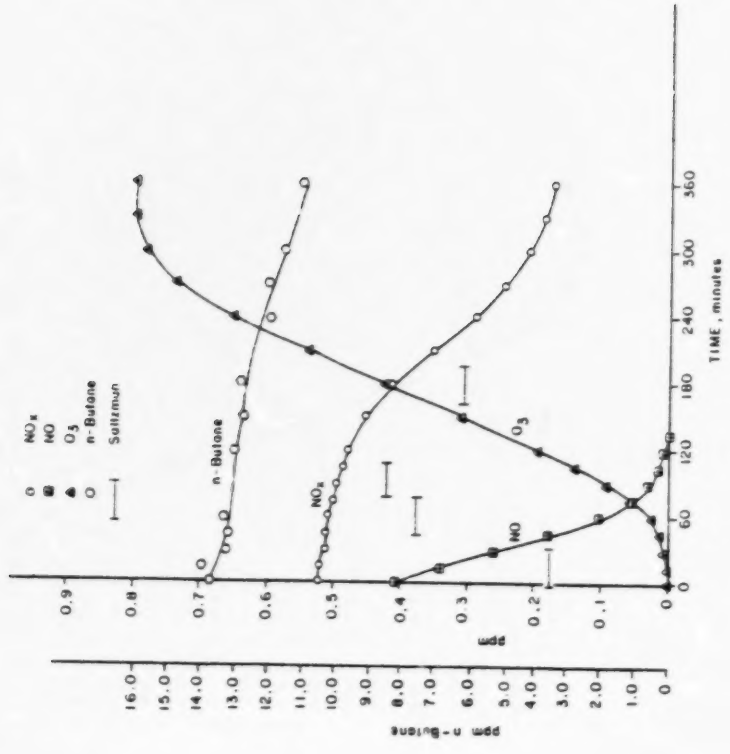

Figure A-43. Reaction profiles of 14.0 ppm n-butane-NO_x system.

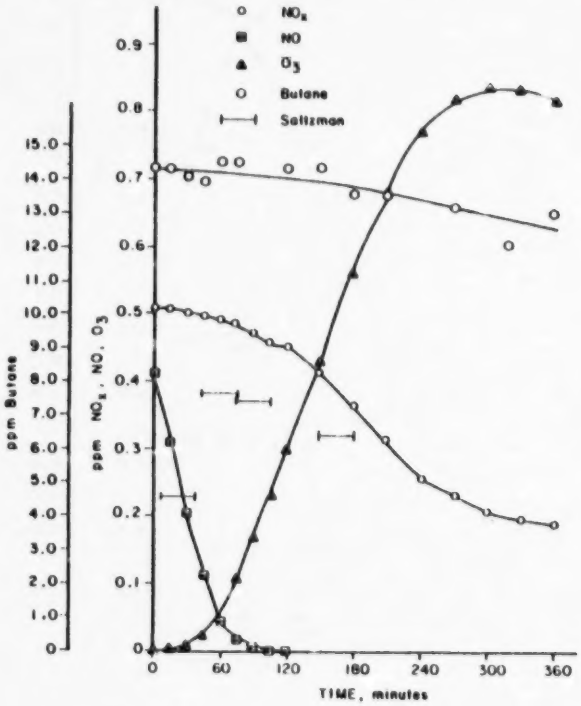

Figure A-44. Reaction profiles of 14.3 ppm n-butane-NO_x system.

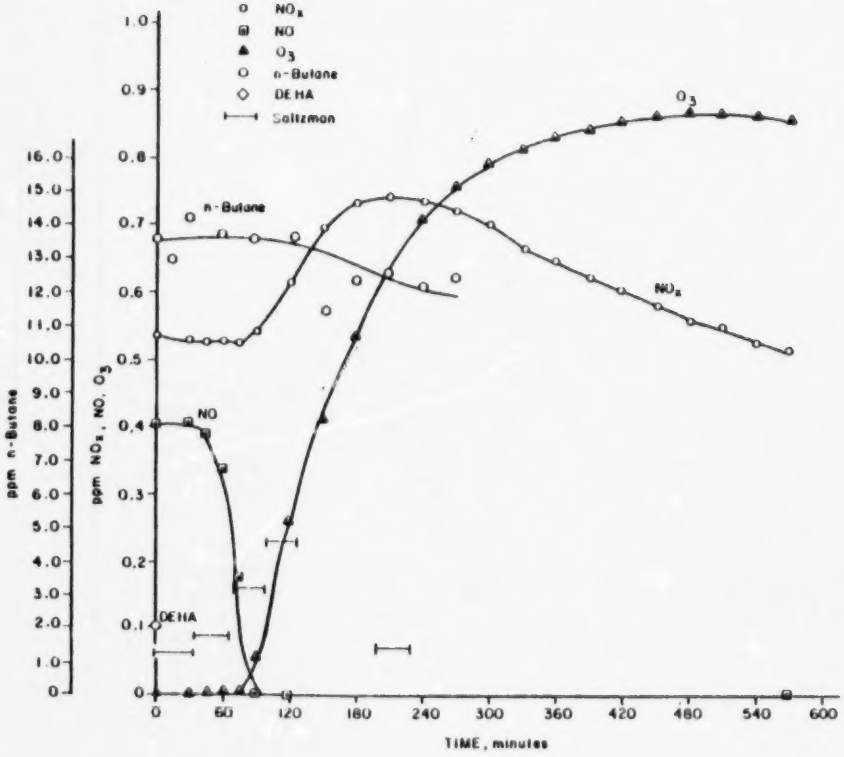

Figure A-45. Reaction profiles of 13.6 ppm n-butane-NO_x-DEHA system.

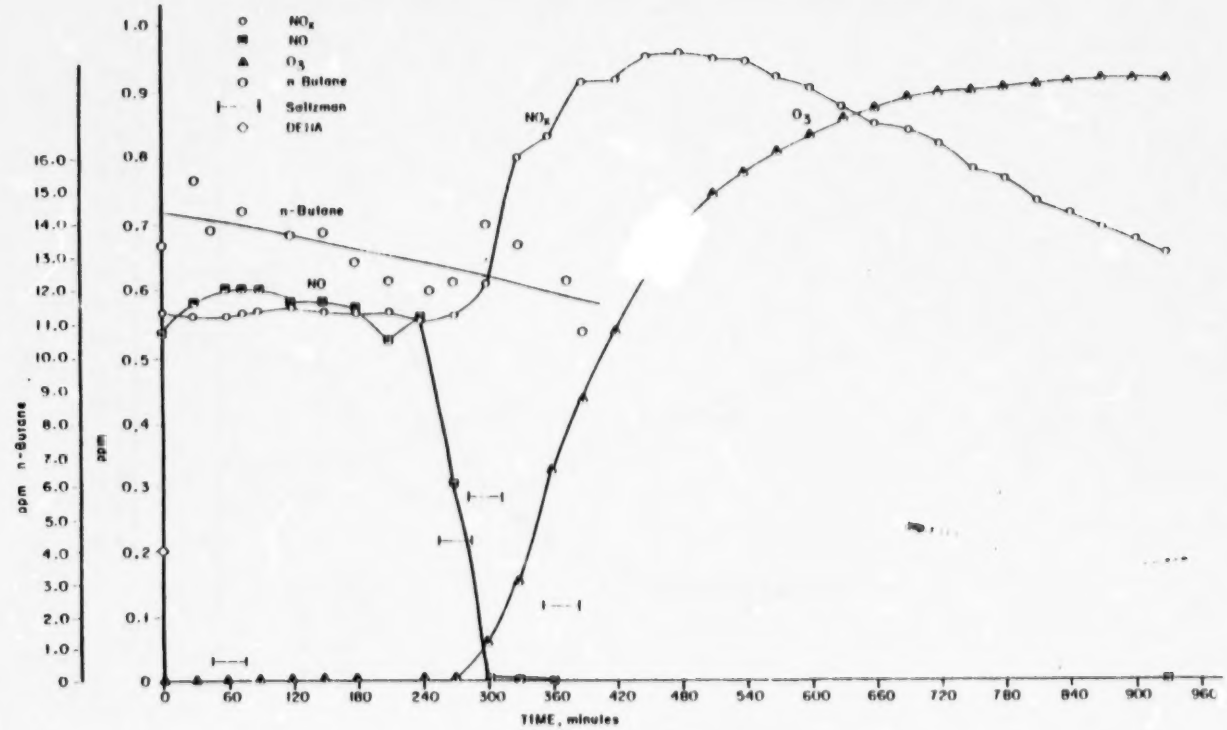

Figure A-46. Reaction profiles of 13.5 ppm n-butane-NO_x-DEHA system.

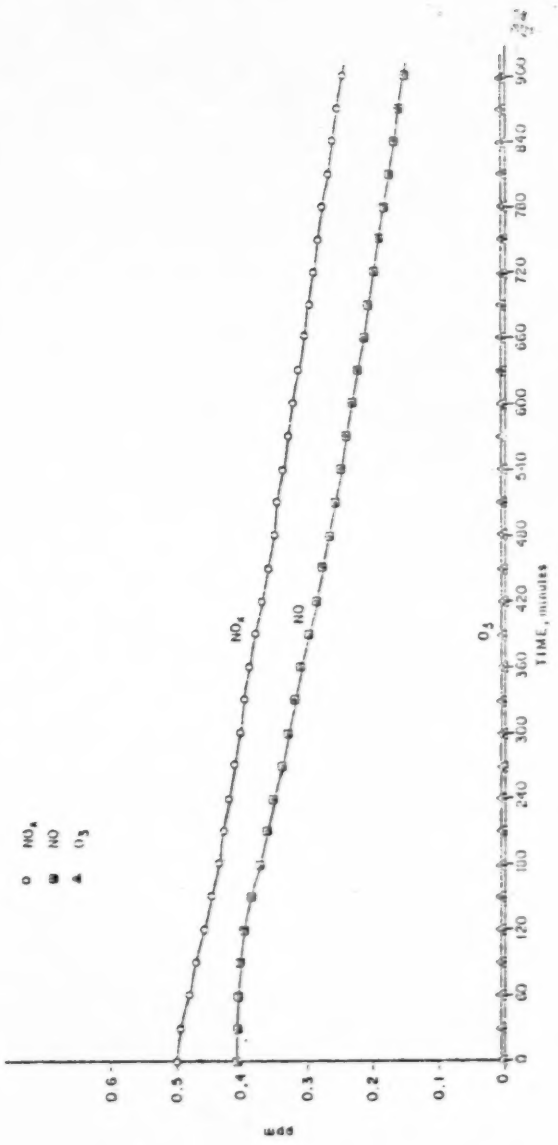

Figure A-47. Reaction profiles of NO_x system.